MEASUREMENTS OF CRITICAL SHEAR STRESS FOR ENTRAINING FINE SEDIMENTS IN A BOUNDARY LAYER

by

Vito A. Vanoni

Professor of Hydraulics

Final Report to

U. S. Public Health Service

Research Grant RG-6915

W. M. Keck Laboratory of Hydraulics and Water Resources
Division of Engineering and Applied Science
California Institute of Technology
Pasadena, California

Report No. KH-R-7

May 1964

TABLE OF CONTENTS

LIST OF FIGURES

LIST OF TABLES

ABSTRACT

Experiments were made in a flume 15-3/8 in. wide by 12 ft long to determine the shear stress for critical motion of fine sediment in a growing boundary layer. Determinations were made for two sediments, a quartz sand with geometric mean sieve size of 0.102 mm and glass beads with geometric mean sedimentation diameter of 0.037 mm.

The intensity of sediment motion was judged from the frequency of bursts of motion over a small area varying from 7 to 18 mm in diameter. When the burst frequency fell between 1/3 and 1 burst per second, critical conditions for inception of motion were considered to obtain.

Values of shear velocity, u_*, and bed shear stress, τ_o, for turbulent flow were determined from measured velocity profile data by essentially two methods. In the first the slope, N, of a straight line fitted to a semi-logarithmic graph of velocity profile data was used in Eq. (8) to obtain u_*. In the other, values of point velocity, u, at a distance of .03 ft from the bed was substituted into the logarithmic equation for velocity distribution at a smooth wall, Eq. (5), to obtain u_*. The data obtained from Eq. (8) and plotted on Fig. 14a show wider scatter than those calculated from Eq. (5) and plotted on Fig. 14b. The data obtained by means of Eq. (5) are considered the more reliable and are presented on a complete Shields diagram in Fig. 15.

Measurements of Critical Shear Stress for Entraining Fine Sediments in a Boundary Layer

by

Vito A. Vanoni

1. Introduction

Many studies have been made of the entrainment of sediment particles resting on the bed of a stream. These have been mostly concerned with relatively coarse sediments with particle sizes in excess of about 0.20 mm. The objective of the present study is to extend the data on entrainment to sediments with smaller particle sizes.

The study of entrainment of finer particles is of interest to the operation of settling tanks commonly used to remove solids from water. The turbid water is introduced at one end of the settling tank and allowed to flow slowly through the tank so solid particles can settle to the bottom and be removed. Particles which settle to the bed may also be reentrained by the flow in the tank and be carried away in the effluent, thus reducing the efficiency of the tank.

The friction developed at the bed of a settling tank retards only a relatively thin layer of the flow, known as the boundary layer. A normal stream such as a river differs from flow in a tank in that bed friction retards the flow over its entire depth. In order to simulate flow in a settling tank, the present studies were made in a flume in which the inflow had a nearly uniform velocity and was almost free of turbulence. As the flow proceeded into the flume, the boundary layer developed and increased in thickness as one would expect to occur in a settling tank. Experiments were made with two sediments, a quartz sand with geometric mean size of 0.102 mm and glass beads with geometric mean diameter of 0.037 mm.

2. Previous Studies

The problem of particle entrainment is an old one and was studied as long ago as early in the 19th century.* The most significant modern

*See Leliavsky, "An Introduction to Fluvial Hydraulics," Constable and Co., Ltd., London, 1955, for a historical resumé of subject.

work is that of Shields (1)**, who expressed his results by the equation,

$$\frac{\tau_c}{(\gamma_s - \gamma) d_s} = f\left(\frac{u_{*c} d_s}{\nu}\right) \qquad (1)$$

where τ_c is the value of the shear stress at the bed under which motion of particles begins, γ_s and γ are the specific weights of the sediment grains and fluid respectively, d_s is the characteristic size of the grains, $u_{*c} = \sqrt{\frac{\tau_c}{\rho}}$ is the so-called critical value of the shear velocity, ρ is the mass density of the fluid, and ν is the kinematic viscosity of the fluid. The dimensionless parameter $\tau_c / (\gamma_s - \gamma) d_s$ will be called the critical Shields parameter or the dimensionless critical shear stress, and the quantity $u_{*c} d_s / \nu$ is the critical value of the well-known boundary Reynolds number. When these quantities are written with the noncritical value τ_o of the shear stress, they will be called the Shields parameter or dimensionless shear stress and the boundary Reynolds number, respectively. Shields's results in which he determined the function $f(\frac{u_{*c} d_s}{\nu})$ are shown in Fig. 1. In his original paper, Shields did not show a curve for the function but indicated it by a shaded area. The curve shown for the figure was introduced by Rouse (2). The auxiliary scale with inclined lines added by the writer facilitates the determination of τ_c once d_s, γ_s / γ and ν are specified.

Shields's experiments were made in a flume with fully-developed velocity profiles and with the bed covered with an artificially flattened bed of sediment. He determined the bed shear stress, τ_o, from measured velocity profiles and Eq. (8) as explained below. The critical shear stress was taken as the value of the shear stress, τ_o, that would give zero transport rate and was determined by extrapolating the curve of transport rate. The representative size d_s was taken as the median sieve size, that is, the sieve size for which 50 per cent by weight of the material was finer or coarser. The sediments used covered a wide range of specific weights and varied in median size from about 0.4 mm to 3.4 mm.

** Numbers in parenthesis indicate item number in the bibliography.

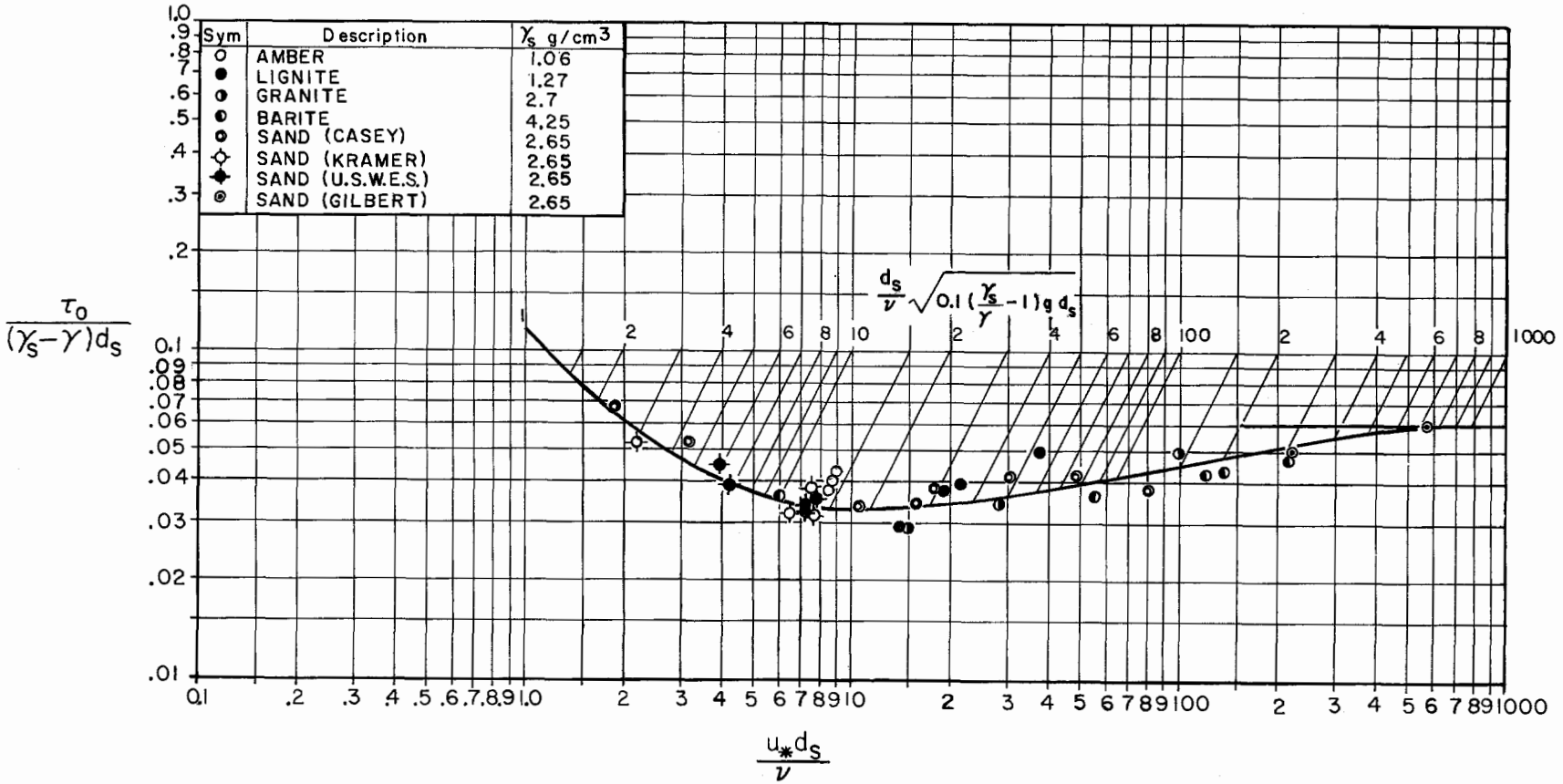

Fig. 1. Shields diagram for critical shear stress (ref. 1).

White (3) determined the critical shear stress for several sediments under conditions of completely developed laminar flow, laminar boundary layer flow, and turbulent boundary layer flow. From his results with the laminar flow, he obtained for $u_* d_s / \nu$ less than 3.5,

$$\frac{\tau_c}{(\gamma_s - \gamma) d_s} = 0.18 \tan \theta \qquad (2)$$

where θ is the angle of repose of the sediment immersed in the liquid. Since according to White tan θ is about unity, the results gave a Shields parameter of about 0.18, as compared to about 0.03 to 0.06 obtained by Shields. From the experiments with turbulent boundary layer flows, White found that τ_c was about one-half of that for a laminar flow. This was explained by the fact that in a turbulent flow, fluctuations occur in the velocity and stress near the bed so that intermittent values of the stress can exceed the mean value and cause motion even when the mean value is less than enough to move the sediment. White's results for turbulent boundary layers give values of Shields parameter of about 0.10, compared to Shields's results in Fig. 1 of from 0.03 to 0.06 depending on the boundary Reynolds number. This discrepancy was attributed to the more intense turbulence in the flows with fully-developed velocity profiles which Shields used, and it is not viewed as a disagreement between the two studies. The main discrepancy between the results of White and Shields is that Shields found that the parameter $\tau_c / (\gamma_s - \gamma) d_s$ reached a minimum value for $u_* d_s / \nu$ in the neighborhood of 10, while White found no such relation. He found that as long as the boundary layer was laminar, the Shields parameter had a constant value of about 0.18, and that when the flow in the boundary layer was turbulent the value reduced to about 0.10 but did not vary with boundary Reynolds number.

Kramer (4) studied the entrainment problem in flumes with fully-developed velocity profiles with the objective of selecting sediments suitable for use in movable-bed hydraulic models. In hydraulic models the sediment movement of the prototype must be simulated without formation of excessively large ripples or dunes which produce abnormally high friction in the model. Kramer defined three rates of sediment movement which he termed 1) weak movement, 2) medium movement, and

3) general movement. As noted by Shields, Kramer's "weak movement" corresponds closely to Shields's critical condition. Kramer's definition of weak movement is that a few or several of the smallest sand particles are in motion in isolated spots in small enough numbers that those moving over any small area of, say, one square centimeter, can be counted. The data points in Fig. 1 showing Kramer's results are for weak movement as are those for results of the U. S. Waterways Experiment Station, (USWES) (5). The experiments of both Kramer and USWES, like those of Shields, were made in flumes with uniform flow. The sediments used were sands with median sizes ranging from 0. 2 mm to 4 mm and with geometric standard deviation of sizes varying roughly from 1. 3 to 2. 3.

3. Apparatus and Procedure

A. Flume Circuit.

A photograph of the flume and circulating system used in the experiments is shown in Fig. 2 and a dimensioned sketch of the system is shown in Fig. 3. The flume which forms the working section of the apparatus is 15-3/8 in. wide, 17 in. deep, and 12 ft long. The structural support for the flume is of steel and very rigid, so deflections under load are negligible. The bed of the flume was set horizontally for all experiments. As shown in Fig. 4, the flume sides are of glass, and the bottom is made of a smooth hard plastic material known commercially as "Formica" and used commonly for kitchen counters. This material was cemented to 3/4-in. thick plywood which is in turn cemented to the structural steel bottom of the channel. The two 1-in. diameter steel rails on the top members of the flume run for the full length of the working section, and support the instrument carriage. This carriage is shown at the downstream end of the working section in Fig. 2.

The water is discharged from the flume into the end well, and then into a 6-in. pipe through an 8-in. gate valve, and into the reservoir, which is 6 ft wide and 6 ft long. The gate valve is used to throttle the flow and thus to regulate the flow depth in the working section. A vertical pump, the electric motor for which is shown over the reservoir in Fig. 2, recirculates the water through the 6-in. pipeline, also shown in Figs. 2 and 3. A venturi meter with inlet and throat diameters of 6. 109 in. and 3. 437 in. ,

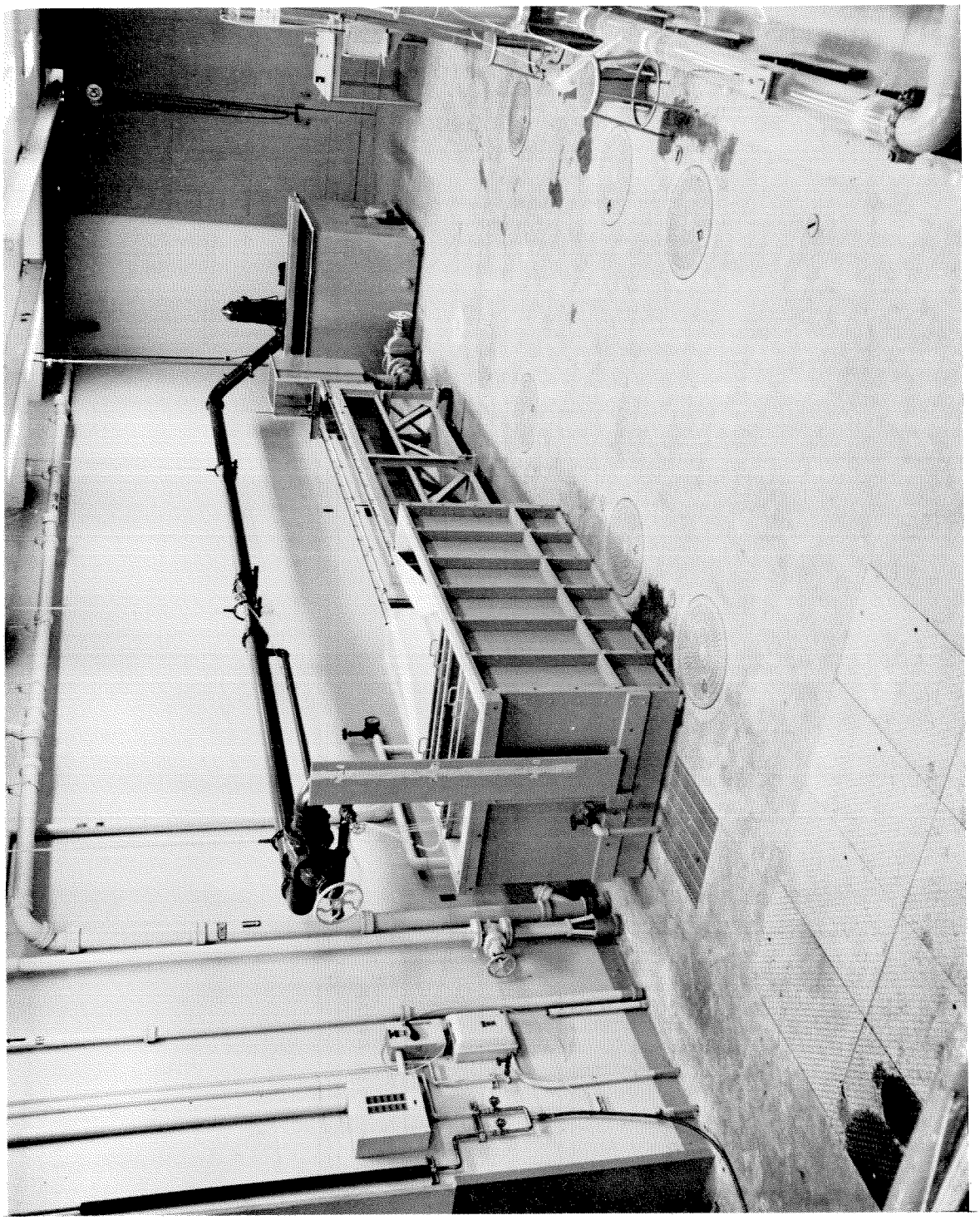

Fig. 2. General view of apparatus.

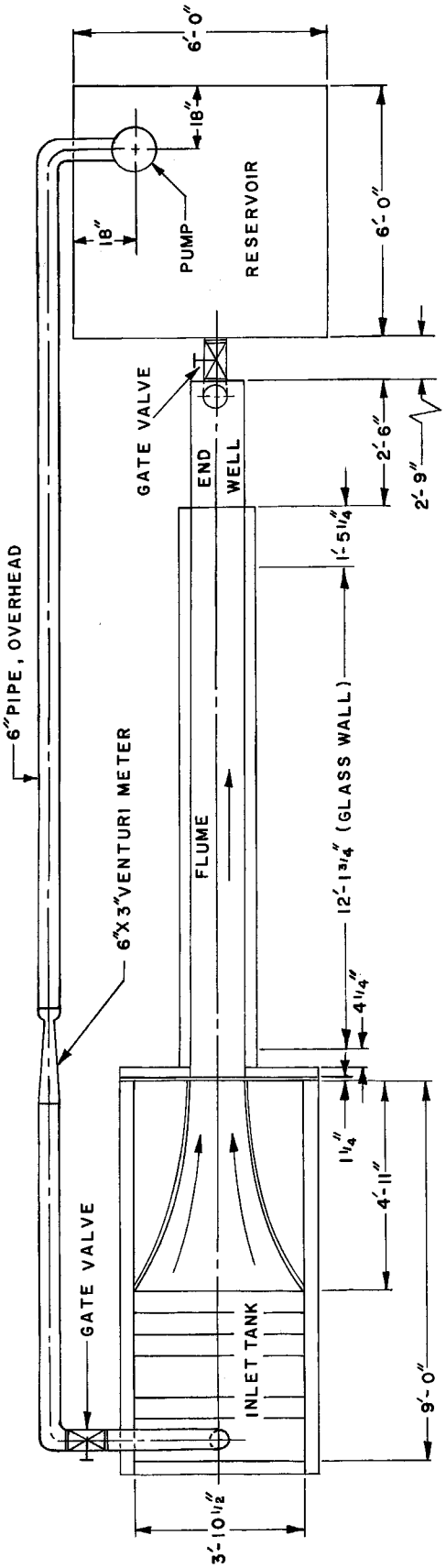

Fig. 3. Plan view of flow system.

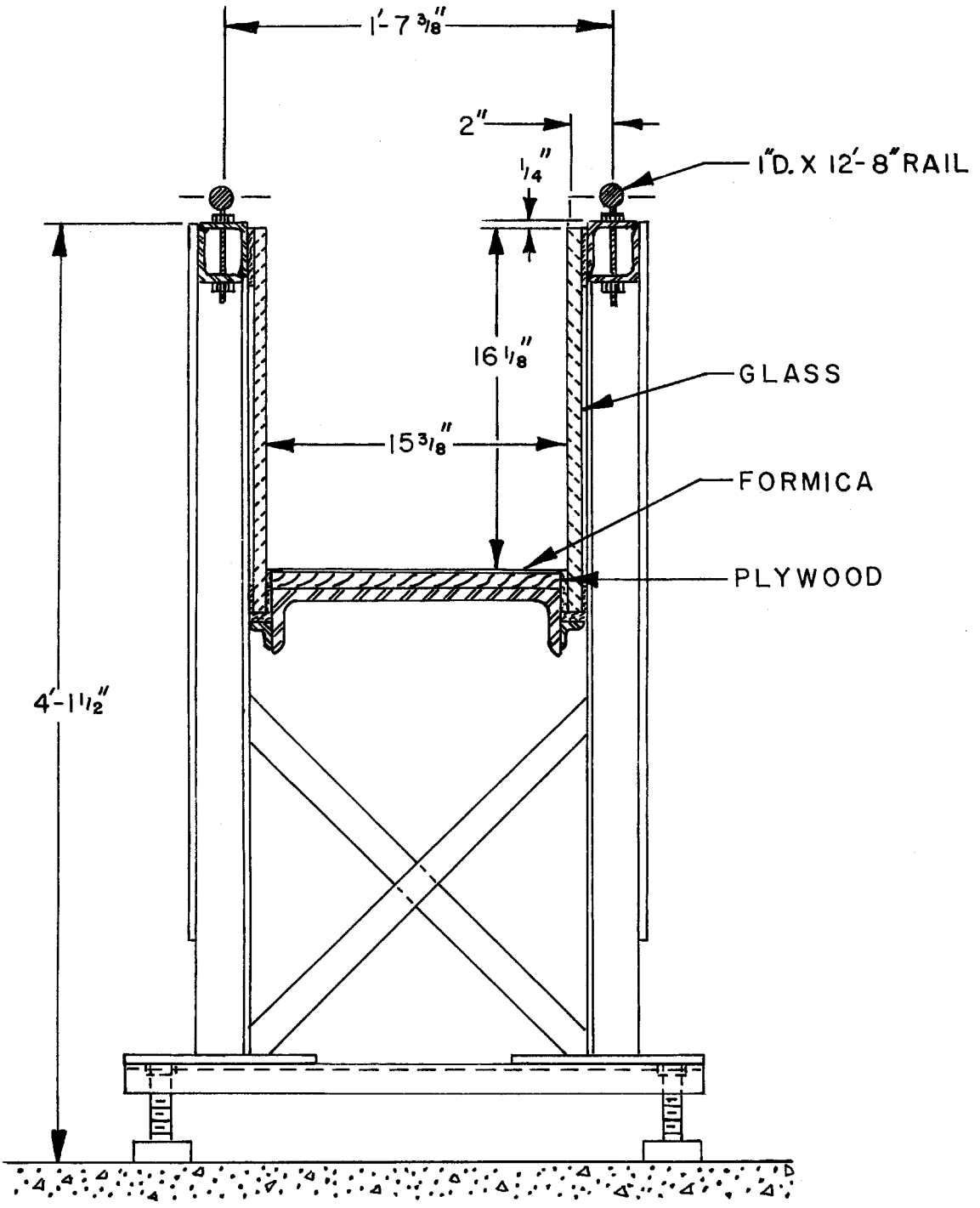

Fig. 4. Cross section of flume.

respectively, was used to meter the flow. The differential head on the meter was read with an air-water manometer reading to 0.001 of a foot. The meter was calibrated volumetrically in the Hydrodynamics Laboratory to an accuracy of well within 1 percent. The 6-in. gate valve shown at the left side of Fig. 2 was used to regulate the discharge.

The inlet tank shown at the left of Figs. 2 and 3 is shown in detail in Fig. 5. The tank which is of waterproof plywood painted on the inside with three coats of epoxy enamel, is 3 ft 10-1/2 in. wide, 9 ft long, and 33 in. deep. Water enters the tank through 312 holes in a manifold, as shown in Fig. 5. The water then passes through two baffles spaced 6 in. apart and occupying the entire cross section of the tank. These baffles are made of galvanized sheet metal about 1/16 in. thick which is perforated with 3/16-in. diameter holes as shown in Fig. 5 spaced 1/4 in. apart in lines 1/4 in. apart. Following the sheet metal baffles are three turbulence-damping screens spaced 6 in. apart. These screens are of monel metal wire .018 in. in diameter woven with 32 square meshes per inch.

Downstream from the screens the water enters a nozzle about 5 ft long which gradually reduces the flow cross section to that of the working section, which is 15-3/8 in. wide and of depth which can be selected. This nozzle is geometrically similar to the one on the 12-in. low-turbulence water tunnel (6) in the Laboratory, except that the top surface was omitted. The water tunnel nozzle was designed to give a monotonically increasing velocity along any stream tube by a method proposed by Tsien (7).

B. Position, Depth, and Velocity Measurements.

As described previously, the instrument carriage ran the full length of the flume on two rails. In addition, the instrument holder was on a smaller carriage that ran transverse to the flow and the instrument holder itself could be raised and lowered by means of a rack and pinion. Thus, with this device an instrument could be positioned anywhere in the flume. The two horizontal coordinates of position were read from scales on the flume and instrument carriage. The elevation coordinate was read to 0.001 of a ft from a vernier scale on the instrument holder.

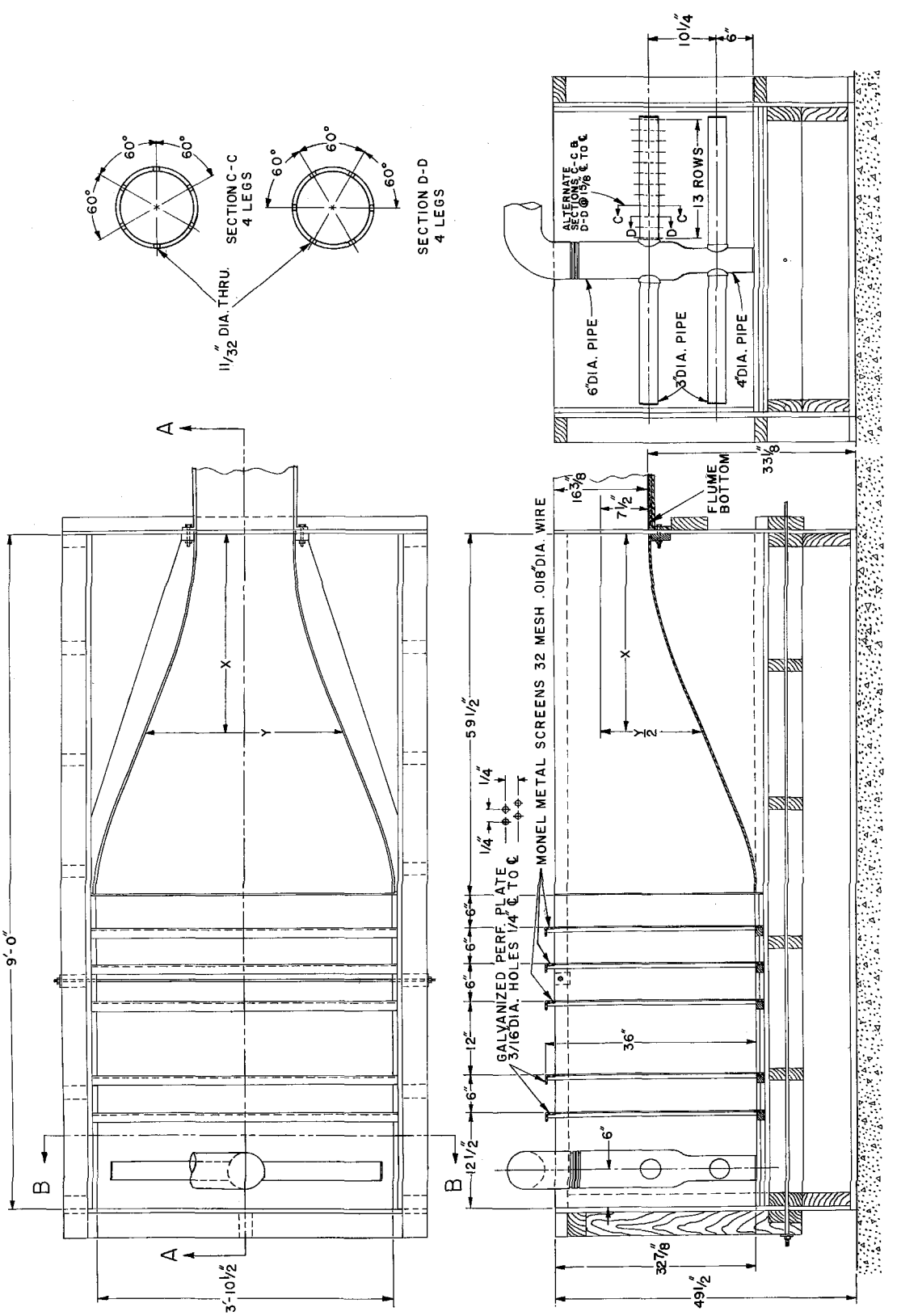

Fig. 5. Details of inlet tank for flume.

The water depth was determined by point gage as the difference in gage reading of the water surface and flume bottom. Since the rails for the instrument carriage were horizontal, the point gage readings were actually elevations above an arbitrary datum.

Most point velocities within the flow were measured by pitot tube and a few were measured by a miniature current meter. Some surface velocities were determined by measuring the time for a surface float to traverse a distance of 3 ft. In order to compare velocities measured by different methods, the 3 ft travel of the floats was selected so its mid-point was located over the point where velocities were measured by pitot tube and current meter.

In measurements with pitot tubes, separate total head and static head tubes were used. This made it possible to keep the tubes small and thus to minimize the flow disturbances which they created. The total head tubes were used singly or in a rake as shown in the sketch of Fig. 6a and at the extreme left of Fig. 7. The single total head tubes were the same as one unit of the rake. Most of the static head measurements were made with the tube shown in Fig. 6b, and a few were made with the one shown in Fig. 6c. During measurements the static head tube was fixed in position several inches to the side of the total head tube and sufficiently above the bed so the field of its disturbance was isolated from the total head tubes and the bed.

The velocity head at the position of the tip of a total head tube was determined as the difference in the total head recorded by the tube and the static head. These heads were measured either with a two-pot micromanometer or the five-pot micromanometer shown in Fig. 7. This device has five pots 1-1/2 in. inside diameter and 3 in. high, spaced 2-1/4 in. apart. It makes possible the simultaneous measurement of four total heads and the common static head. The position of the water surface in each pot was read by standard machinists micrometers with scales 1 in. long graduated to 0.001 of an in. A pointed brass rod on the end of each micrometer shaft was brought down to the water surface until contact was made and the micrometer reading was then noted. Since the datums of the micrometers were not exactly at the same elevation it was necessary to determine their relative elevation. To do this the flow was stopped and the water in the

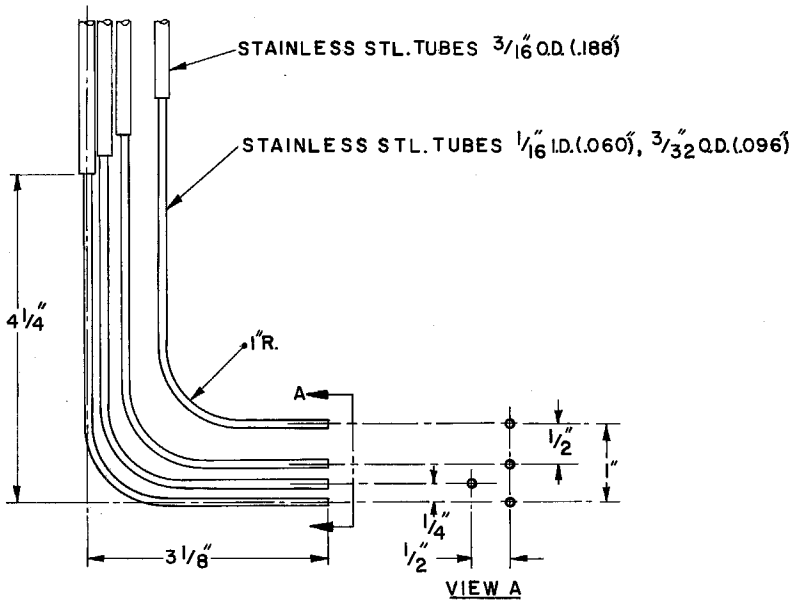

(a) RAKE OF TOTAL HEAD TUBES

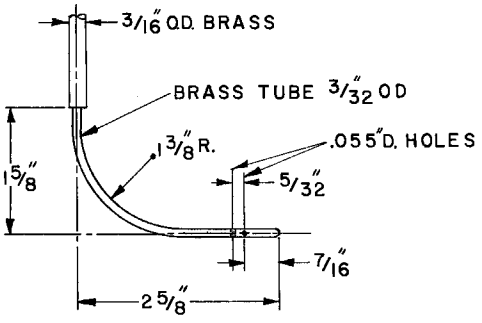

(b) 3/32 INCH STATIC TUBE

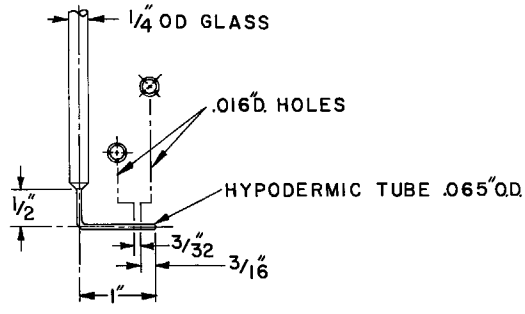

(c) .065 INCH STATIC TUBE

Fig. 6. Sketch of pitot tubes used to measure velocity.

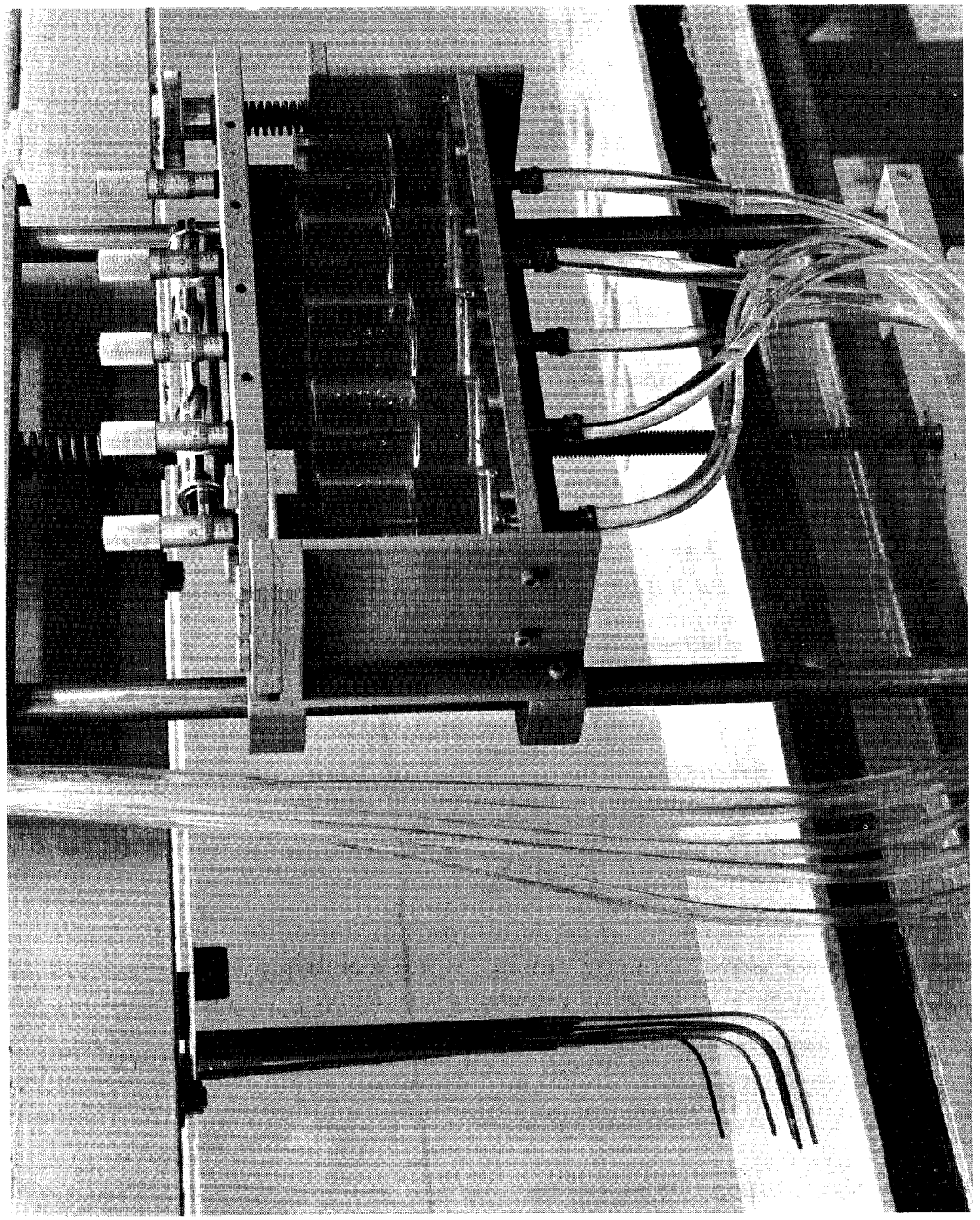

Fig. 7. Five-pot micromanometer used to measure velocity.

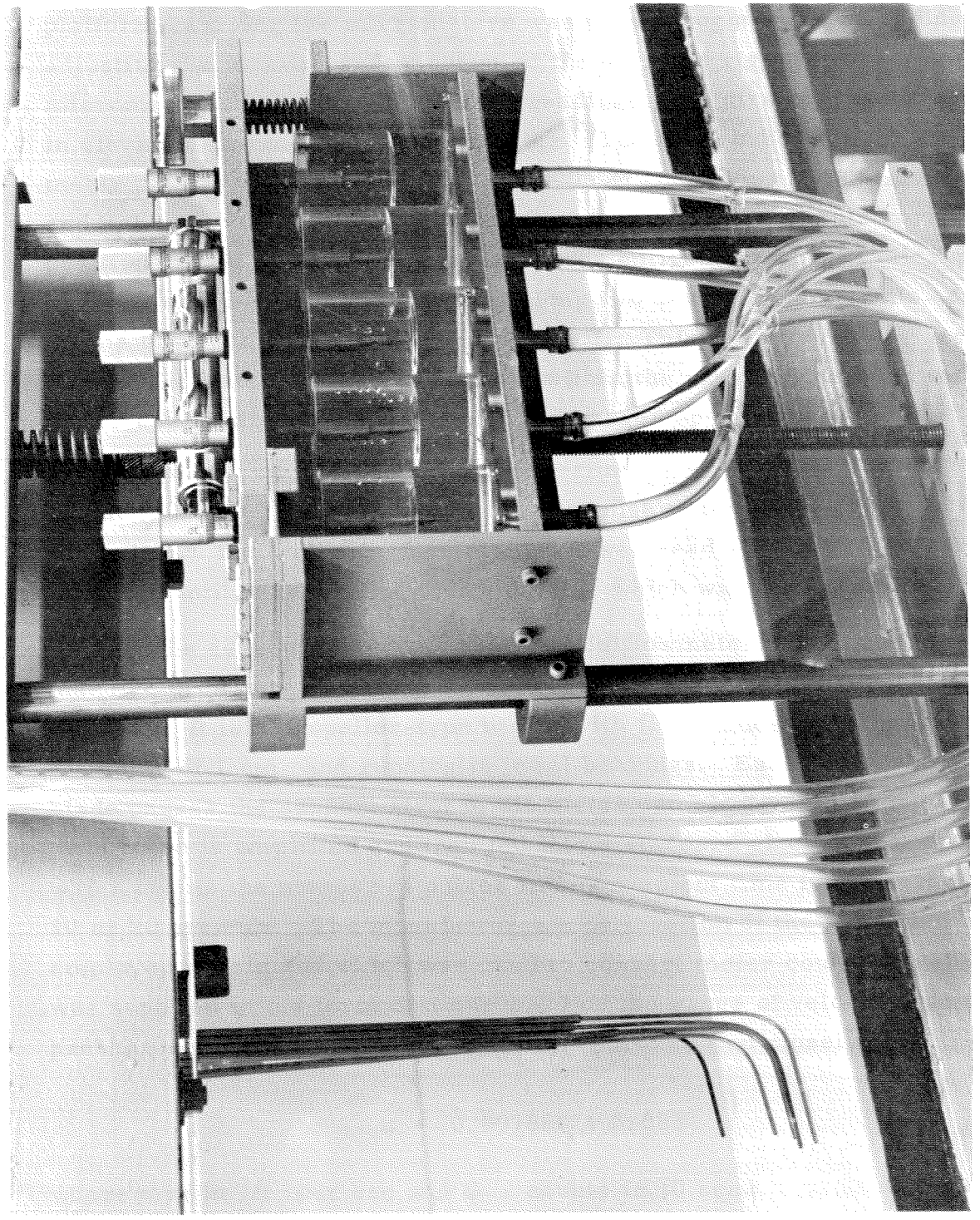

Fig. 7. Five-pot micromanometer used to measure velocity.

pots was allowed to come to a common elevation. The level bubble on the platform carrying the micrometers was then brought to zero reading by adjusting the leveling screw shown at the extreme right of Fig. 7 and each micrometer was read. These zero readings gave directly the difference in elevation datum of each micrometer. The level bubble on the micrometer platform had a sensitivity of 0.005 of an in. per ft per division and was used to detect any movement of the platform from its horizontal position and to reset it if necessary. The entire assembly of micrometers and pots could be moved vertically along two 1-in. diameter rails, by means of a lead screw as shown in Fig. 7. This adjustment was necessary to keep the water surface in the pots within the range of the 1-in. micrometer scales when the flow depth was changed appreciably.

The velocity heads in these experiments were small, ranging from about 0.002 to 0.02 of a ft, and the response of the water level in the pots was slow. The water surface elevation was read at intervals of several minutes until it reached a constant value which was then recorded.

The current meter used was a Miniflowmeter probe AWE 183/1 manufactured by Armstrong-Whitworth Aircraft, Ltd., of Gloucester, England. It is a propeller-type meter with five blades, with propeller diameter of 1 cm, and running in jewel bearings. Each time a propeller blade passes the support strut of the meter, an electric pulse is generated. This pulse is amplified and then fed into a standard electronic counter which counts the number of pulses in a convenient time interval such as 10 or 20 seconds. The manufacturer's calibration of the particular meter employed herein and which was used to convert meter counts to velocity was supplied in the form of a curve. For the range of velocities in the present experiments this curve can be approximated closely by

$$u = 0.00188C + 0.083$$

where u is in ft per sec and C is counts in 10 sec.

The floats used to measure surface velocities were introduced well upstream from where they were timed, so they had come up to speed in the measuring reach. They were timed with an electric interval timer reading to 0.1 sec and operating off the 60 cycle per sec frequency of the electric power system.

A comparison of velocities measured in the same flows by the three methods is shown in Table 1.

Table 1

Velocities at Centerline of Flume Measured by Pitot Tube, Current Meter, and Surface Floats

Run No.	Water Depth ft	Dist. above Bottom ft	Vel. ft/sec		
			By Pitot Tube	By Current Meter	Surface Vel. by Float
23	0.404	0.368	0.797	0.768	-
23	0.404	0.404	-	-	0.785
24	0.404	0.365	0.733	0.737	-
24	0.404	0.404	-	-	0.725
26	0.404	0.380	0.761	0.742	-
26	0.404	0.404		-	0.750

In the three experiments referred to in Table 1 the boundary layer at the measuring points was less than 0.15 of a ft thick so that the measurements were made in that part of the cross section where the velocity was uniform. This means that the velocity at the surface was essentially the same as at the points within the flow where measurements were made with pitot tubes and the current meter. Therefore, the differences in the three measurements can be attributed to the errors inherent in the devices used. The maximum deviation between measurements amounted to less than 4 percent and occurred in Run 23 between the pitot tube and current meter measurements.

Fig. 8 shows velocity profile measurements for Run 24 on the centerline of the flume 4.4 ft. from the inlet. The one surface float velocity is also shown. The agreement between pitot tube and current meter measurements is good where the velocity is uniform. In the boundary layer where the velocity gradient is high, the two measurements differ appreciably and give substantially different velocity gradients. Since the current meter is large (1 cm in diameter) it cannot be expected to give

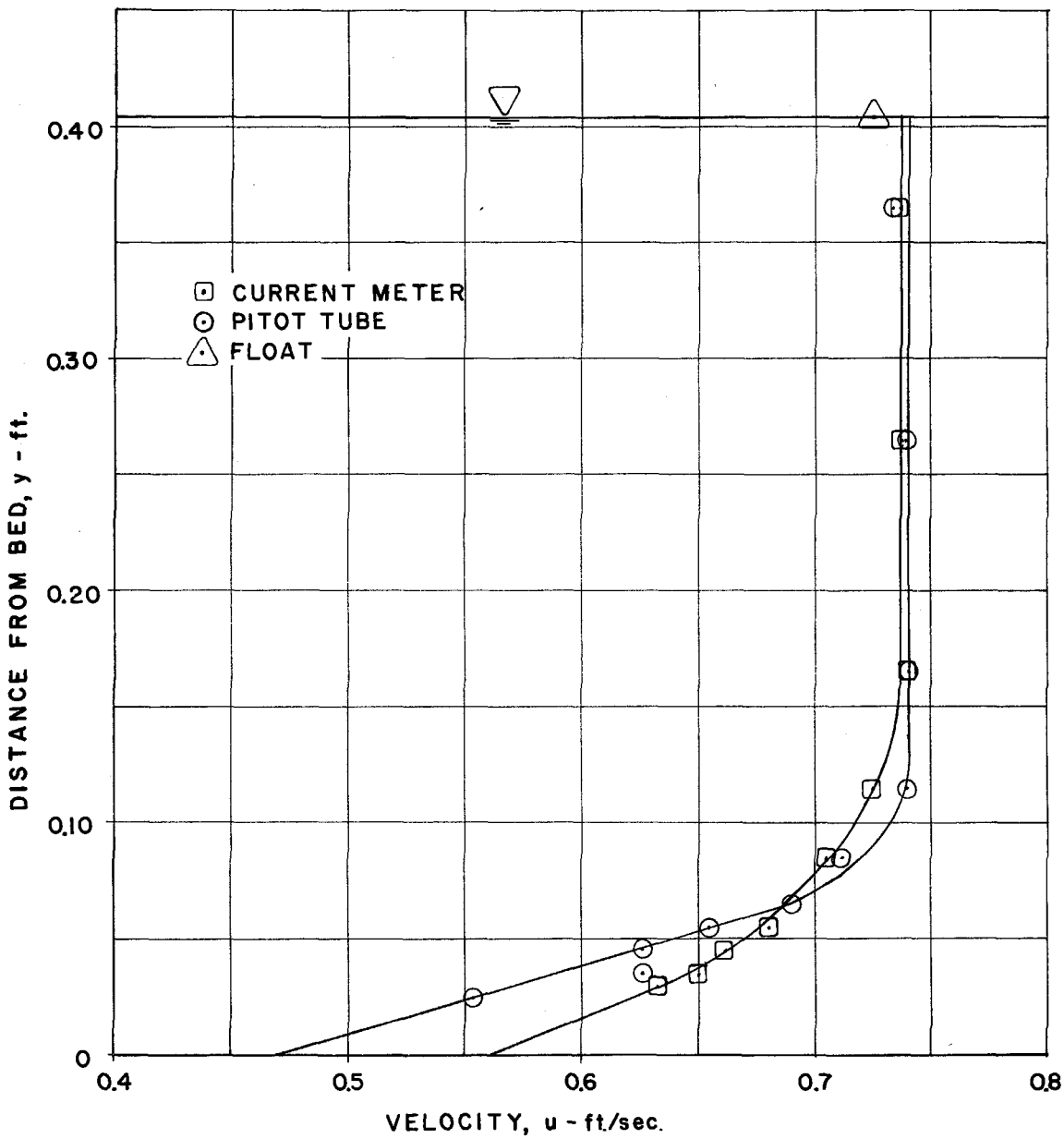

Fig. 8. Velocity profile in run 24 on centerline of flume at station 4.4 ft comparing measurements by current meter, pitot tube and surface float.

good results where the velocity changes rapidly with position. Therefore, all velocity measurements near the bed which were used to determine shear stress were made with pitot tubes.

C. Preparation of Sediment Bed.

All except some preliminary experiments were made with a layer of sediment on the bed of uniform thickness of about 3/8 in. The sediment was flattened out carefully with a view to making the bed surface correspond closely to a plane. This was done with a scraper made of a straight metal bar carried on a wood carriage which slid along the rails used to support the instrument carriage. The bed remained in this flattened condition during all observations of sediment movement reported herein.

D. Observation of Bed Movement.

In order to facilitate detailed observations of the motion of sediment grains on the flume bed, an optical apparatus was used with a field of view ranging from 7 to 18 mm in diameter. This apparatus, shown diagramatically in Fig. 9, proved to be very convenient for observing the details of motion on the bed. It not only enlarged the grains in the field of view, but it made possible concentration of attention on a specific small area without the distraction of activity in neighboring areas usually experienced in visual observations with the naked eye.

When the threshold conditions for beginning of motion were approached one observed intermittent motion of sediment in any small area. This motion occurred in bursts or gusts produced by the turbulence in the flow near the bed and covered areas that were at least an order of magnitude larger than the viewing area used in these observations. Many grains were moved simultaneously in each burst of motion. By observing a small area with the apparatus of Fig. 9, one could count the number of bursts in a convenient time interval, and for the 0.102 mm sand it was also possible to estimate the average number of grains in motion in the field of view during the bursts. These data then formed a basis for judging when critical conditions for motion were reached. Table 2 gives data on

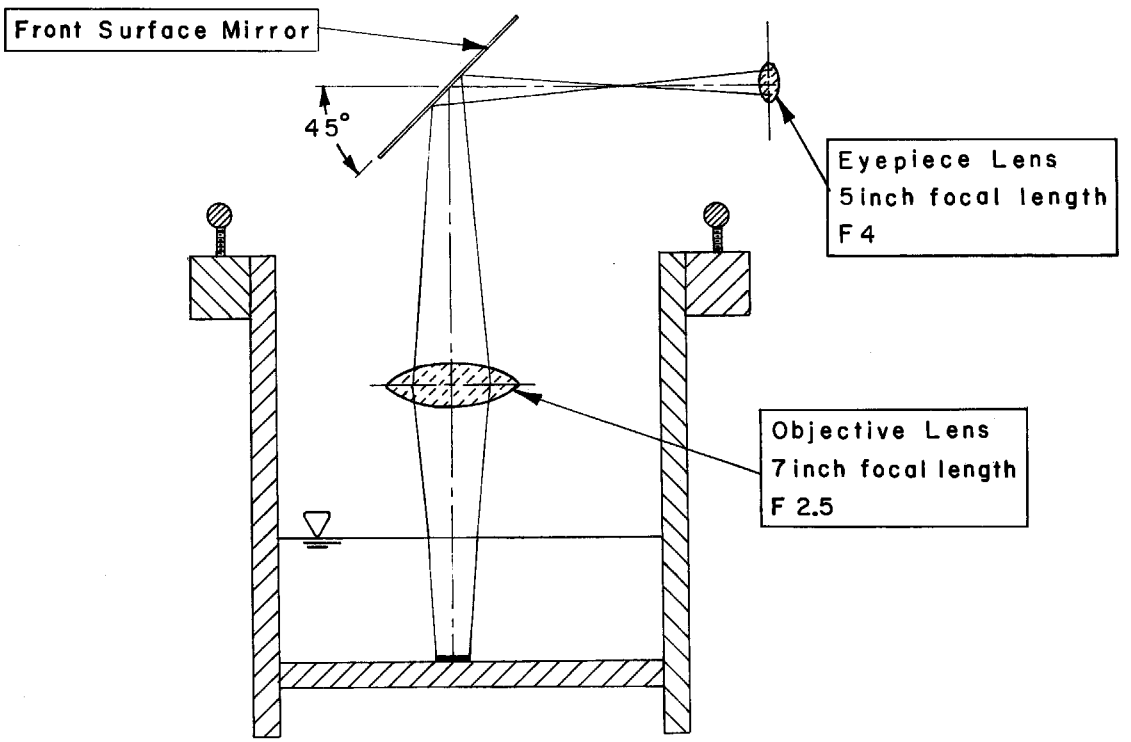

Fig. 9. Optical apparatus used to observe bed.

burst frequency and average number of grains in motion in the field of view during a typical burst for the 0. 102 mm sand.

Table 2

Burst Frequency and Approximate Number of Grains Moved per Burst On a Bed of 0. 102 mm Sand

Run No.	R-7	31-B	31-C	R-3	R-11	R-4	R-13	R-12
Distance from Inlet, ft	10	11	11	10	10	10	10	10
Bursts per Sec.	1/7	1/7	1/4	1/3	1/3	2/3	2/3	1
No. of Grains in Motion	5	5 to 10	40	10	10	20	30	40
Field Diameter mm	8	18	18	8	8	8	8	8

It is clear from Table 2 that burst frequency and number of grains moved are strongly correlated. Because of this and because the estimate of number of grains moved is very approximate and difficult to make, and hence of limited value, the burst frequency was adopted as a measure of rate of sediment movement. The criteria used for sediment movement in terms of burst frequency are listed in Table 3. As noted when the burst frequency fell between 1/3 and 1 per sec. ,threshold conditions for critical motion were considered to exist. This appears to agree with Kramer's (4) definition of "weak movement" which also agrees with determinations by Shields (1) of the critical or threshold conditions.

In experiments in which conditions were near critical, more movement was observed at the beginning of the experiment than later on. In some cases, motion actually ceased after a period of an hour or two. Apparently grains which were left in unstable positions by the leveling process, or which are very easy to move are the ones which moved at the beginning of these experiments. These grains continued to move until they found a stable position on the bed or were swept out of the flume. Because

of this phenomenon an adjustment period of about an hour or more was allowed before observations of intensity of motion were made.

Table 3
Criteria for Incipient Sediment Movement
In Terms of Frequency of Bursts of Movement

Burst Frequency Burst per Sec.	Rate of Movement
Less than 1/10	Negligible
1/10 to 1/3	Small
1/3 to 1	Critical
Larger than 1	General

E. Visual Observations of Flow.

The boundary layer near the inlet was thin and laminar. In a region farther into the flume the flow commenced to show intermittent turbulence and finally still further downstream the flow became permanently turbulent. The boundary layer grew in thickness with distance from the inlet.

The state of turbulence and approximate thickness of the boundary layer were observed using potassium permanganate as a dye to disclose the fluid motion. Crystals of the dye were dropped into the flow. As they fell they left a thin wake of dyed water which remained as a vertical line in the region of uniform velocity and deformed toward the flume inlet in the boundary layer. The distance from the bed of the flume up to the point where these dye lines departed from a straight line is the boundary layer thickness and could be estimated by reading a scale placed on the outside of the flume wall. The dye line above the boundary layer always remained intact, indicating the absence of turbulence in this zone. The line also remained intact in a laminar boundary layer but as soon as turbulence developed in the boundary layer, the lines deformed drastically, the dye was dispersed in a distance of about a foot, and the line vanished. In this manner it was very easy to detect the onset and presence of turbulence.

4. Results of Experiments

A. Outline of Experiments.

Two series of experiments were made, each series being made with a single sediment. The cumulative size-frequency distributions for these sediments are shown in Fig. 10 on logarithmic probability coordinates along with the geometric mean size, d_g, and the geometric standard deviation, σ_g, for the two materials. It will be observed that both materials are very well sorted. The 0.102 mm sand used in the first series of experiments was a natural quartz sand obtained from a local foundry supply firm. It had well-rounded grains and a specific gravity of 2.65. Its size distribution was determined by sieve analysis. The glass beads were obtained from the Minnesota Mining and Manufacturing Company and are listed as Material No. 500 in their catalog. The beads are essentially spherical and have a specific gravity of 2.49. Their size distribution was determined by the pipette method in water with a temperature of 23° C. Stokes Law for the fall velocity of small spheres was used to calculate sphere diameter, i.e., sedimentation diameter, from fall velocity observed in the pipette analysis. The pertinent properties of the sediments are summarized in Table 4.

Table 4

Properties of Sediments Used in Experiments

Sediment	Geom. Mean Size d_g - mm	Size Scale	Geom. Std. Deviation σ_g	Specific Gravity
Sand	0.102	Sieve Size	1.14	2.65
Glass Beads	0.037	Sedimentation Dia.	1.19	2.49

The outline of the experiments is best set forth by Table 5, which summarizes the main observations made in the experiments. It is seen that flow depths ranged between 0.269 and 0.706 ft, and discharge varied between 0.152 and 0.900 cu ft per sec, giving mean velocities ranging between approximately 0.4 and 1.0 ft per sec.

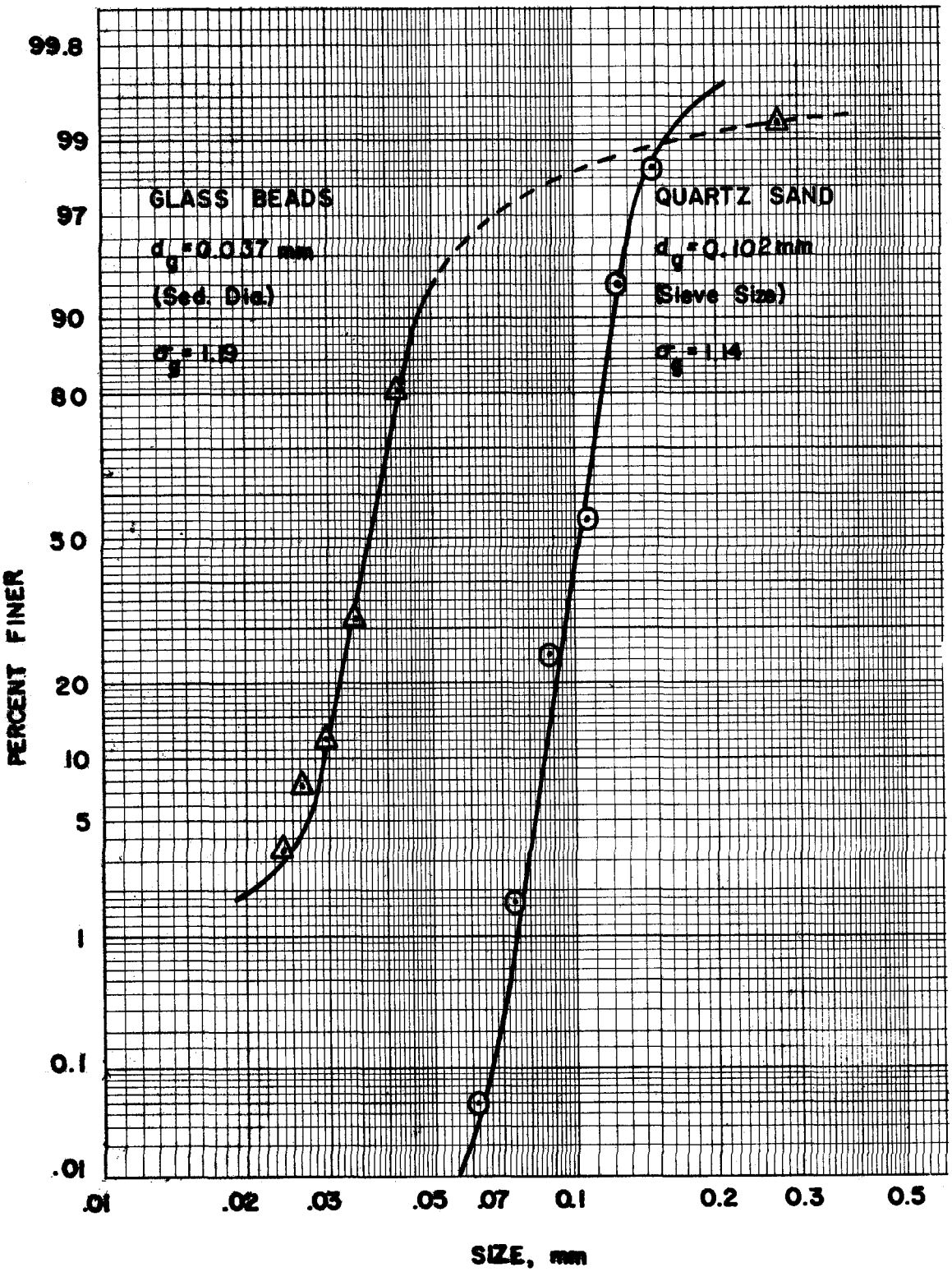

Fig. 10. Size-frequency distribution of two sediments used in experiments.

Table 5

Summary of Data

1	2	3	4	5	6	7	8	9	10	11	12
Run No.	Depth d - ft	Discharge Q-ft³/sec	Water Temp. °C	Sta. of Trans. ft	Sta. of Observ. ft	Particle Motion(1) Burst/sec	Particle Motion(1) No. of grains	Condition of Bdry. Layer	Bdr. Layer Thickness δ - ft	Undist. Velocity u_o, ft/sec	Intens. of Motion
Series I, 0.102 mm Sand											
R-1	0.391	0.190	21.5	5	1	none	none	lam.	0.045	0.388	none
	0.391				5	none	none	trans.	0.050	0.421	none
	0.391				10	none	none	turb.	0.085	0.502	none
R-1A	0.391	0.258	21.5	6.5	10	none	none	turb.	0.120	0.585	none
R-2	0.391	0.290	21.5	5	1	none		lam.	0.050	0.612	none
					5	rare		trans.	0.060	0.638	negligible
					10	rare	1 to 2	turb.	0.110	0.660	negligible
R-3	0.391	0.358		4	1	none		lam.	0.045	0.748	none
					5	rare		trans.	0.065	0.788	negligible
					10	1/3	10	turb.	0.150	0.810	small
R-4	0.391	0.410	21.5	5	1	none		lam.	0.055	0.856	none
					5	-	-	trans.	0.065	0.890	small
					10	2/3	20	turb.	0.130	0.923	critical
R-5	0.391	0.295	22.0	6	10	rare	3 to 4	turb.	0.130	0.617	negligible
R-6	0.391	0.308	22.0	5.5	10	rare	1 to 2	turb.	0.125	0.700	negligible
R-7	0.391	0.355	22.0	4.5	10	1/7	5	turb.	0.115	0.780	small
R-8	0.391	0.288	22.0	6	10	none	none	turb.	0.135	0.635	none
R-11	0.306	0.300	21.5	2	10	1/3	10	turb.	0.120	0.861	small
R-12	0.306	0.335	21.5	-	10	1	40	turb.	0.170	1.027	critical
R-13	0.306	0.320	21.5	3	10	2/3	30	turb.	0.130	0.934	critical
R-15	0.301	0.370	21.5	-	1	2/3	80	turb.	0.065	0.962	critical
					5	(2)		turb.	0.115	1.075	general
					10	(2)		turb.	0.140	1.13	general
23A	0.404	0.369	21.5	-	4.4			trans.	0.140	0.796	small
24A	0.404	0.369	22.0	-	4.4			trans.	0.140	0.738	small
31B	0.706	0.620	21.5	4	11	1/7		turb.	0.150	0.747	small
31C	0.706	0.720	21.5	3	11	1/4		turb.	0.210	0.863	small
31D	0.706	0.900	21.5	-	11			turb.	0.215	1.07	general
Series II, 0.037 mm Glass Beads											
I	0.269	0.152	22.5	-	3	none		lam.	0.050	0.471	none
					7	1/30		trans.	0.045	0.508	negligible
					10	1/10 to 1/5		turb.	0.090	0.502	small
II	0.269	0.208	22.5	5	2	none		lam.	0.040	0.656	none
					5	1/100		trans.	0.050	0.662	negligible
					7	1/5		turb.	0.090	0.686	small
					9	1		turb.	0.100	0.707	critical
					10	1		turb.	0.120	0.714	critical
III	0.412	0.155	21.5	8.5	10	1/40		turb.	0.060	0.341	negligible
IV	0.531	0.260	22.0	8	8	1/5		trans.	0.095	0.415	small
					9	1/5		turb.	0.115	0.420	small
					10	1/3		turb.	0.115	0.420	small
V	0.269	0.173	22.5	8	8	rare		trans.	0.050	0.577	negligible
					9	-		turb.	0.080	0.580	small
					10	-		turb.	0.090	0.585	small

(1) 8 mm field for Series I except that in Runs 31B-D field was 18 mm.
7 mm field for Runs I, II, and III, 18 mm for Run IV, 9 mm for Run V.

(2) Dunes developed soon after experiment started.

B. Flow Pattern in Flume.

The depth of flow along the flume was measured carefully with the point gage in each experiment. In no instance did the depth change more than .001 of a ft over the 12 ft length of the flume. The water depth for each run is listed in column 2 of Table 5.

Several surveys of the velocity in the flume cross section showed some slight asymmetry in the flow. The nature of this is shown in Fig. 11 where three velocity profiles at station 10 of Run R-3 have been plotted. It will be noted that the profiles on centerline and 0.25 ft left of center (looking downstream) agree closely while the one 0.25 ft right of center shows lower velocities than the other two. Similar asymmetries were observed at other stations and in some other runs. These are not believed to have any important effect on the results.

All of the velocity profiles for which data are recorded in Table 5 were made at the centerline of the flume.

Fig. 12 shows velocity profiles at Stations 1, 5, and 10 for each of Runs R-2, R-3, and R-4. These runs have the same flow depth but different discharges and hence different mean velocities. The sand motion increases from none in Run R-2 to critical motion at Station 10 of Run R-4. The figure shows how curves were fitted to the data points and how the free stream velocity u_o, and boundary layer thickness, δ, were obtained. These quantities are tabulated in columns 10 and 11 of Table 5 for all velocity profiles.

The station or distance from the flume inlet at which transition from laminar to turbulent flow occurred is shown in column 5 of Table 5. The position at which transition occurred fluctuated with time over a reach of a foot or more. The positions of transition listed in Table 5 are mean values determined according to the judgment of the observer. The presence of turbulence or the existence of laminar flow was determined by observing dye lines as described in part 3. The condition of flow in the boundary layer determined in this manner is noted in column 9 of Table 5.

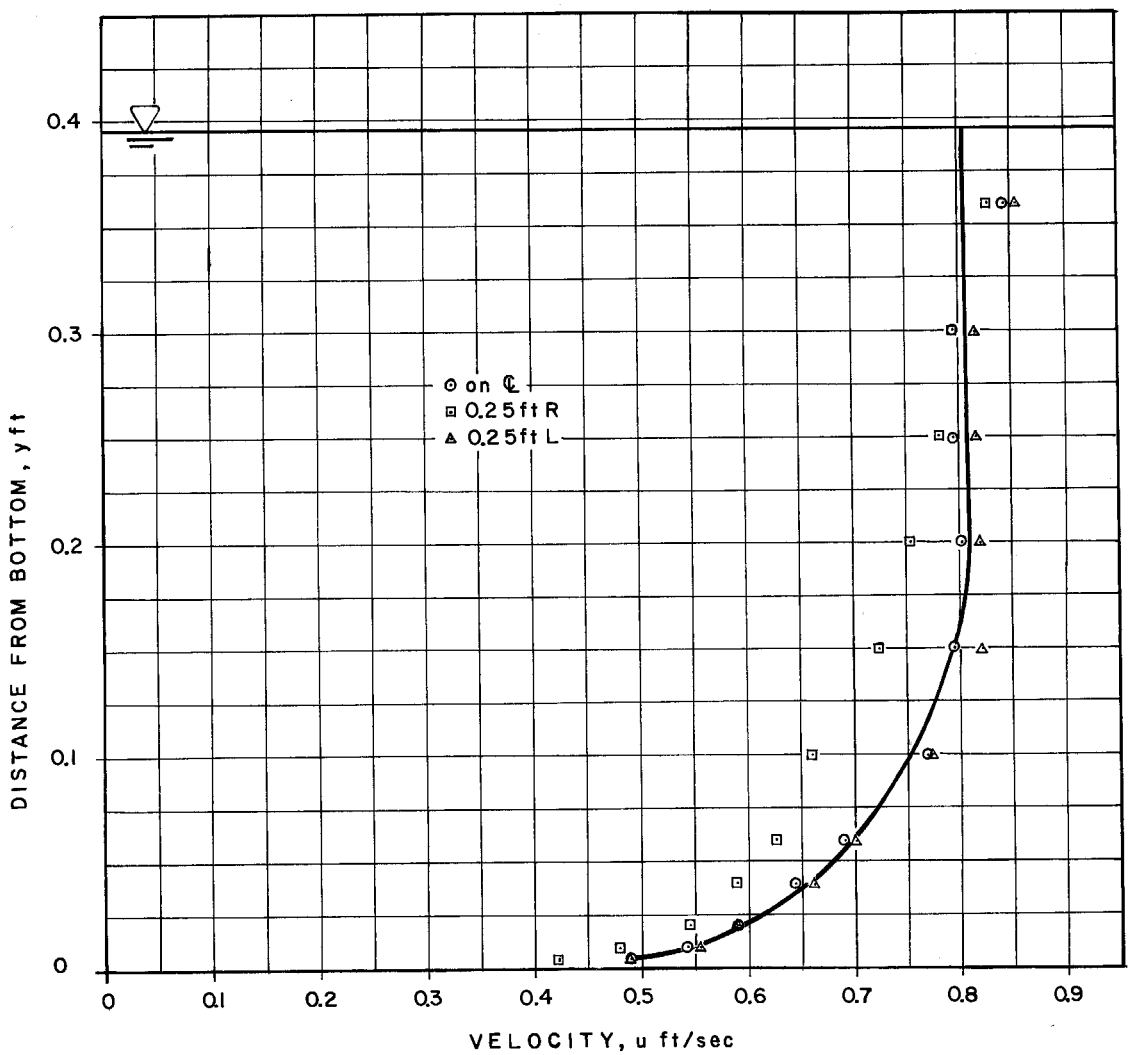

Fig. 11. Velocity profiles in run R-3 at station 10.

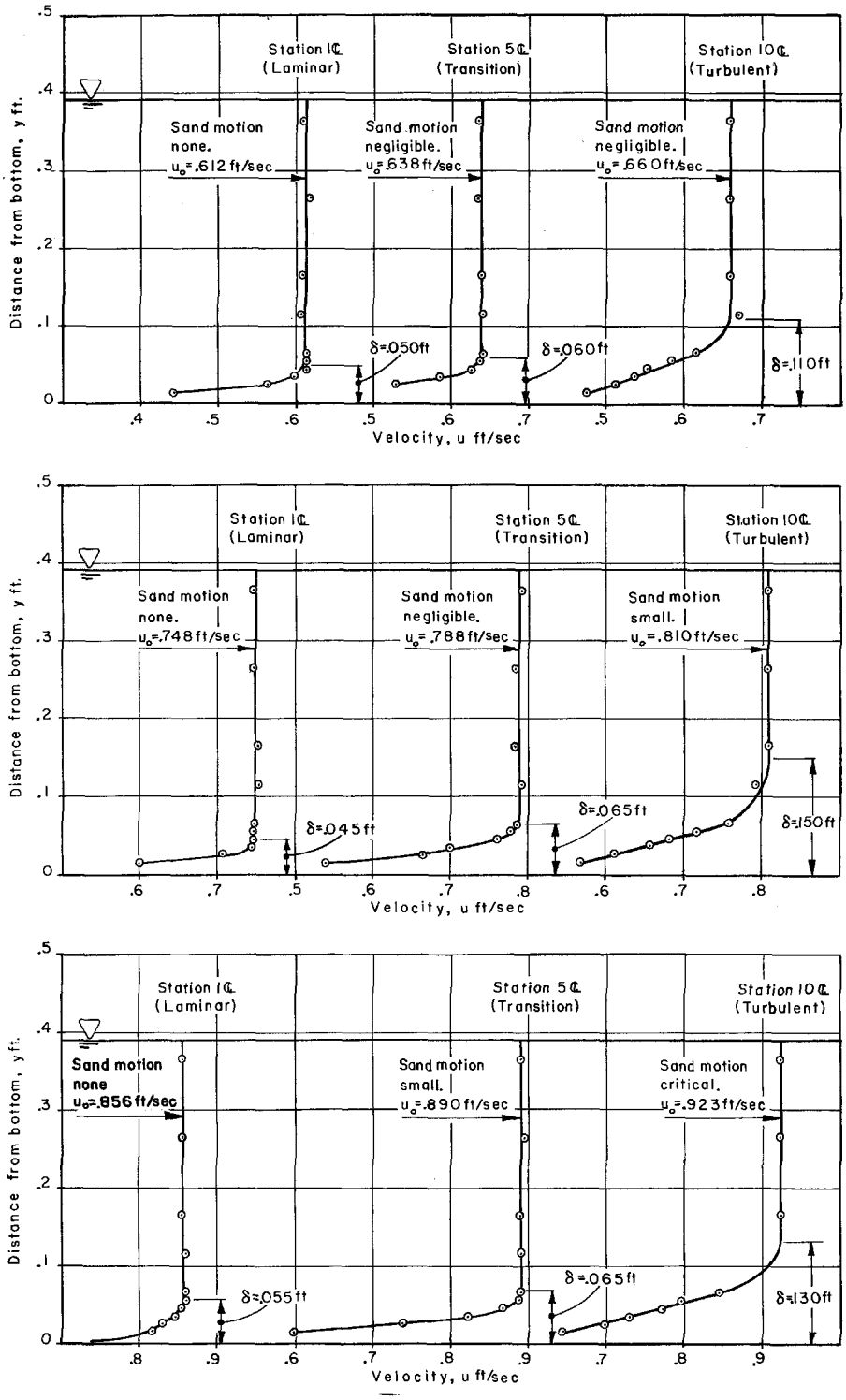

Fig. 12. Velocity profiles at three stations showing growth of boundary layer.

C. Observations of Sediment Movement.

Observations of sediment movement were made on a small area using the optical system of Fig. 9. The detailed observations of the frequency of bursts of turbulence which moved grains in the small area and the average number of grains moved per burst are recorded in columns 7 and 8, respectively, of Table 5. The equivalent adjective description of intensity of motion is listed in column 12 of the table. In cases where burst frequency is not recorded but adjective descriptions appear, the latter was reconstructed from descriptive notes made during the experiment.

D. Shear Velocity and Dimensionless Parameters.

In the present experiments, shear velocity and shear stress were calculated only for turbulent flow and no attempt was made to determine these quantities for flow in the laminar or transition regions. Several relations are available for making the calculations for turbulent flow.

For the case where the boundary layer thickness, δ, is small compared with the depth, d, one can write

$$Q = u_o (d - \delta_*) (w - 2\delta_*) \tag{3}$$

where Q is the discharge and δ_* is the displacement thickness of the boundary layer defined by

$$\delta_* = \int_o^{\delta} \frac{(u_o - u)}{u_o} dy \tag{4}$$

where u_o is the velocity outside the boundary layer and u is the velocity at distance y from the wall. Eq. (3) assumes that δ_* is the same at the bed and walls. The velocity distribution law for a smooth wall,

$$\frac{u}{u_*} = 5.5 + 5.75 \log \frac{u_* y}{\nu} \tag{5}$$

provides a convenient means of determining u_*. In this equation ν is the kinematic viscosity of the fluid, u_* is the shear velocity given by $u_* = \sqrt{\tau_o/\rho}$, where τ_o is the wall shear stress and ρ is the mass density

of the fluid. Assuming that Eq. (5) applies in the boundary layer, one obtains that at $y = \delta$, $u = u_o$, and one then obtains an expression for $u_o - u$ which can be substituted into Eq. (4) to obtain,

$$\delta_* = \frac{u_* \delta}{0.4 u_o} \tag{6}$$

Now δ_* can be eliminated between Eqs. (3) and (6) to give,

$$\frac{u_*}{u_o} = \frac{0.1}{\delta} \left[2d + w \pm \sqrt{(2d + w)^2 - 8wd \left(1 - \frac{\bar{u}}{u_o}\right)} \right] \tag{7}$$

where $\bar{u} = Q/wd$ is the mean velocity of the flow. By substituting measured values of δ, d, w, $\bar{u}$, and u_o into Eq. (7), one can calculate u_*.

A second way to obtain u_* is by measuring velocities at two or more points in a vertical in the boundary layer. From Eq. (5) one can write,

$$N = \frac{u(y_2) - u(y_1)}{\log y_2/y_1} = 5.75\, u_* \tag{8}$$

where the symbol N has been introduced for convenience. Eq. (8) can be used to calculate u_* from the measurements. In the present experiments several point velocities were measured in the boundary layer as illustrated in Fig. 12. These were then plotted on a graph of u against log y and N was determined as the slope of a line fitted to the points. Such graphs are shown in Fig. 13 for the profiles at Station 10 for Runs R-1 to R-4. The values of N for each turbulent flow profile are shown in Column 6 of Table 6. The shear velocity u_* can also be calculated from Eq. (5) with a measurement of the velocity, u, at one position, y. This calculation can be expedited by rewriting of Eq. (5) in the form,

$$\frac{u}{u_*} + 5.75 \log \frac{u}{u_*} - 5.5 = 5.75 \log \frac{uy}{\nu} \tag{9}$$

This equation can now be plotted on a graph of u/u_* against log uy/ν and the graph used for direct determination of u_*. From one velocity measurement and the fluid temperature one can determine ν and calculate uy/ν,

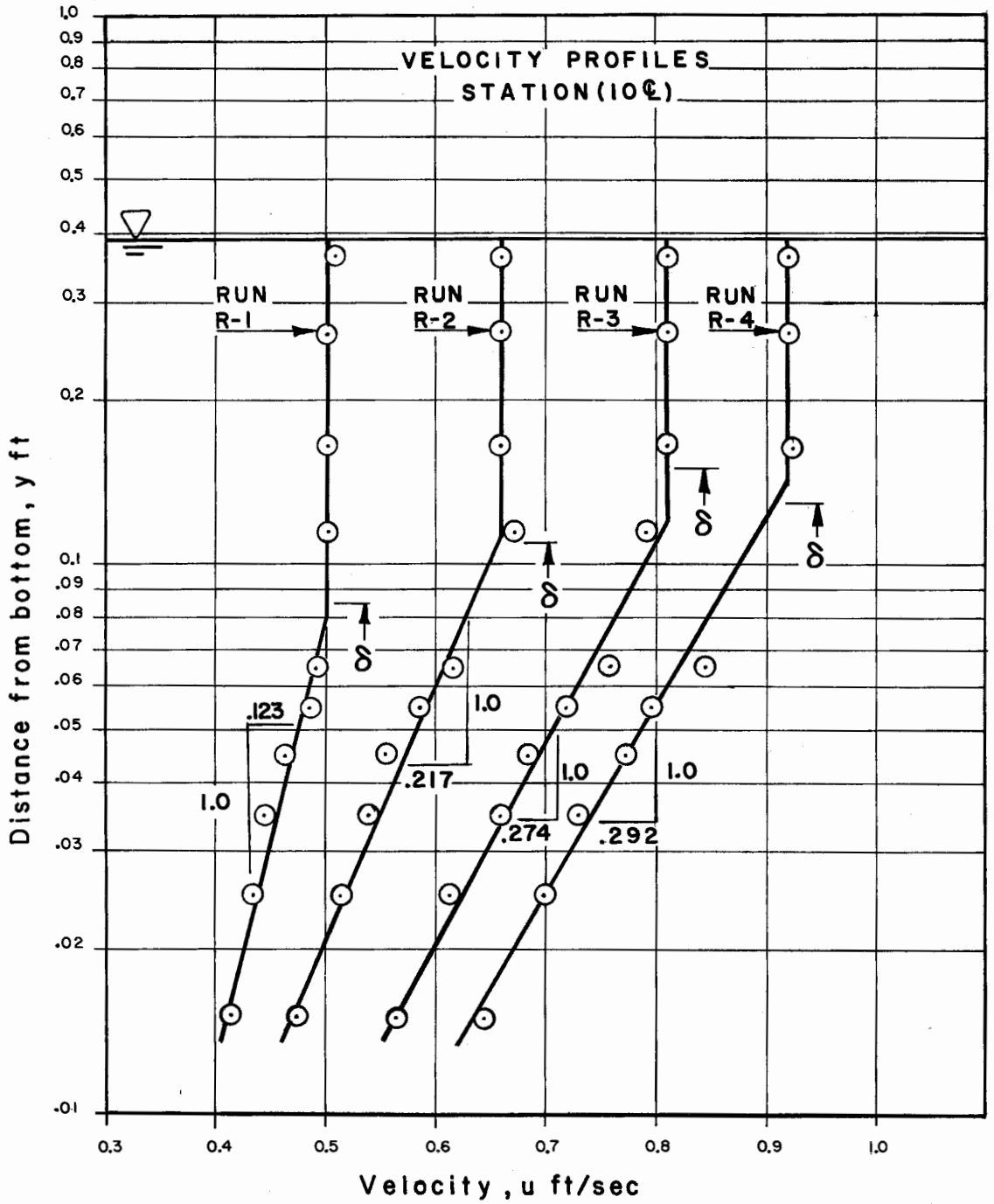

Fig. 13. Semilogarithmic velocity profiles on centerline at station 10.

Table 6

Shear Velocity and Dimensionless Parameters Calculated from Measured Velocities in Turbulent Flows

1	2	3	4	5	6	7	8	9	10	11	12	13	14
Run No.	Station ft	Boundary Layer Thickness δ, ft	Undisturbed Velocity u_o/ft/sec	Vel. at y= 0.03 ft u, ft/sec	Slope of Log. Vel. Profile N, ft/sec	Shear Velocity u_*, ft/sec			$u_* d_s/\nu$		$\frac{\tau_o}{(\gamma_s - \gamma)d_s}$		Intensity of Sediment Motion
						Eq. (8)	Eq. (5)	Eq. (10)	Eq. (8)	Eq. (5)	Eq. (8)	Eq. (5)	
Series I, 0.102 mm Sand													
R-1	10	0.085	0.502	0.448	0.123	0.0214	0.0263	0.0275	0.692	0.849	0.0259	0.0389	none
R-1A	10	0.120	0.585	0.477	0.187	0.0325	0.0288	0.0288	1.04	0.925	0.0595	0.0467	none
R-2	10	0.110	0.660	0.536	0.217	0.0377	0.0319	0.0323	1.21	1.02	0.0799	0.0573	negligible
R-3	10	0.150	0.810	0.647	0.274	0.0477	0.0376	0.0384	1.53	1.21	0.128	0.0797	small
R-4	10	0.130	0.923	0.723	0.292	0.0508	0.0414	0.0420	1.63	1.33	0.145	0.0965	critical
R-5	10	0.130	0.617	0.517	0.160	0.0278	0.0308	0.0313	0.903	1.00	0.0436	0.0535	negligible
R-6	10	0.125	0.700	0.573	0.172	0.0299	0.0338	0.0341	0.972	1.10	0.0503	0.0644	negligible
R-7	10	0.115	0.780	0.657	0.213	0.0370	0.0378	0.0384	1.20	1.22	0.0770	0.0804	small
R-8	10	0.135	0.635	0.533	0.177	0.0308	0.0316	0.0319	1.00	1.03	0.0535	0.0564	none
R-11	10	0.120	0.861	0.753	0.223	0.0386	0.0428	0.0432	1.23	1.36	0.0840	0.103	small
R-12	10	0.170	1.027	0.859	0.210	0.0365	0.0474	0.0482	1.17	1.52	0.0750	0.126	critical
R-13	10	0.130	0.934	0.817	0.217	0.0378	0.0460	0.0464	1.21	1.48	0.0807	0.120	critical
R-15	5	0.115	1.075	0.906	0.335	0.0583	0.0518	0.0529	1.88	1.66	0.191	0.151	general
R-15	10	0.140	1.13	0.918	0.380	0.0661	0.0508	0.0536	2.12	1.63	0.246	0.146	general
31B	11	0.150	0.747	0.597	0.277	0.0482	0.0350	0.0353	1.55	1.12	0.130	0.0690	small
31C	11	0.210	0.863	0.667	0.298	0.0518	0.0387	0.0393	1.66	1.22	0.151	0.0845	small
31D	11	0.215	1.07	0.854	0.263	0.0457	0.0478	0.0485	1.47	1.54	0.118	0.128	general
Series II, 0.037 mm Glass Beads													
I	10	0.090	0.502	0.423	0.223	0.0388	0.0260	0.0261	0.460	0.310	0.261	0.119	small
II	7	0.090	0.686	0.609	0.210	0.0365	0.0355	0.0360	0.432	0.430	0.230	0.218	small
II	9	0.100	0.707	0.622	0.187	0.0327	0.0362	0.0365	0.387	0.428	0.184	0.226	critical
II	10	0.120	0.714	0.626	0.193	0.0336	0.0364	0.0368	0.398	0.432	0.195	0.228	critical
III	10	0.060	0.341	0.305	0.132	0.0231	0.0196	0.0196	0.266	0.226	0.0919	0.0663	negligible
IV	9	0.115	0.420	0.363	0.107	0.0186	0.0227	0.0230	0.216	0.265	0.0595	0.0888	small
IV	10	0.115	0.420	0.338	0.147	0.0256	0.0218	0.0214	0.298	0.249	0.113	0.0782	small
V	9	0.080	0.580	0.533	0.115	0.0200	0.0317	0.0320	0.232	0.378	0.0688	0.173	small
V	10	0.090	0.585	0.530	0.117	0.0204	0.0314	0.0318	0.242	0.367	0.0717	0.170	small

and then enter the graph, read u/u_* and calculate u_* from the known value of u. To calculate u_* by this method the value of u at y = 0.03 ft read from the semilogarithmic graphs of the kind shown in Fig. 13 was used. This value of u for each profile is given in Column 5 of Table 6.

From boundary layer theory* based on the 1/7th power law for the velocity profile, one has for turbulent flow,

$$\frac{u}{u_*} = 8.74\left(\frac{u_* y}{\nu}\right)^{1/7} \qquad (10)$$

This equation also furnishes a means of calculating u_* from one point-measurement of velocity.

Calculations of u_* for turbulent flows were made in four ways, i.e., by means of Eqs. (5), (7), (8), and (10). The results of calculations by Eqs. (5), (8), and (10) are shown in Columns 8, 7, and 9 respectively of Table 6. Values calculated by Eq. (7) turned out to be very erratic and have not been included. It will be noted that there is very good agreement between values of u_* calculated by Eqs. (5) and (10). In calculations with both of these equations the values of u at y = .03 ft listed in Table 6 were used.

The values of u_* calculated by Eq. (8) are not in good agreement with those obtained from Eqs. (5) and (10). The deviations between values calculated by Eqs. (5) and (8) are frequently as much as 10 percent and about one-quarter of them exceed 25 percent. This is attributed to the errors inherent in determining the slope, N, of lines fitted to velocity profile data as illustrated in Fig. 13.

The boundary Reynolds number, $u_* d_s/\nu$ and the dimensionless shear stress $\tau_o/(\gamma_s - \gamma)d_s$ based on u_* and τ_o calculated by Eqs. (5) and (8) are listed in Columns 10 to 13 of Table 6. It will be observed that $u_* d_s/\nu$ always has a value less than 2, indicating that the bed is always hydrodynamically smooth and thus justifying the assumption of smooth wall made tacitly in applying Eq. (5). The data calculated by Eq. (8) are plotted in Fig.14a and those calculated by Eq. (5) appear in Fig. 14b. In calculating

---

* For example, see Streeter,"Fluid Dynamics,"Sec. 9, McGraw-Hill Co., 1960.

these parameters, the sediment size, d_s, was taken as the geometric mean size, d_g, or in other words, the sand size was taken as 0.102 mm and the size of the glass beads was taken as 0.037 mm.

Table 7

Boundary Reynolds Number and Dimensionless Shear Stress for Observed Critical Sediment Movement

Run No.	Sta.	$\frac{u_{*c} d_s}{\nu}$		$\frac{\tau_c}{(\gamma_s - \gamma) d_s}$	
		Sand d_s = 0.037 mm			
		Eq. (8)	Eq. (5)	Eq. (8)	Eq. (5)
R-4	10	1.63	1.33	0.145	0.0965
R-12	10	1.17	1.52	0.0750	0.126
R-13	10	1.21	1.48	0.0807	0.120
		Glass beads d_s = 0.037 mm			
II	9	0.387	0.428	0.184	0.226
II	10	0.398	0.432	0.195	0.228

Table 7 lists the values of the critical boundary Reynolds number, $u_{*c} d_s / \nu$ and dimensionless critical shear stress, $\tau_c / (\gamma_s - \gamma) d_s$ calculated with u_{*c} obtained by two methods. Values of the dimensionless critical shear stress for the sand in which u_{*c} was calculated by Eq. (8) vary as much as 100 percent, and those in which u_{*c} was calculated by Eq. (5) have an extreme variation of about 30 percent. The variations in the two values for the glass beads are much less, but it must be observed that both of these were obtained in one run, i.e., Run II. As has already been observed, the agreement between values of critical shear stress calculated with different equations is not good. However, as can be seen from Table 7, the maximum variation between values of critical shear stress for the sand, calculated by Eqs. (5) and (8) occurs in Run R-12 and is about 70 percent. This is less than the variation of 100 percent between values for Runs R-4 and R-12 calculated from u_* obtained by Eq. (8). Thus it appears that deviation in the dimensionless critical shear stress between runs is of the same order as that resulting from use of different methods of calculating u_* for the same run.

Some of the scatter in the data for critical movement of Fig. 14 is due to unavoidable errors in determining the slope, N, of the velocity profile and the reference velocity, u, at y = .03 ft. The errors in the velocities themselves amount only to a few percent at most, and do not contribute significantly to the scatter. When a line was fitted to velocity profile data to get "N", the slope for best fit and maximum and minimum values of N were also estimated by selecting alternate ways of fitting the lines. At the same time values of u at y = .03 were read from these alternate lines. The maximum values of N obtained in this way were as much as 40 percent larger than the value for best fit recorded in Table 6, and on the average were about 20 percent larger. The minimum values were as much as 16 percent smaller than the values in Table 6, but averaged only 4 percent smaller. The values of u at y = .03 ft read from the curves with maximum and minimum slope, N, varied only 4 percent or less from those listed in Table 6. These variations in u contribute a like variation to u_* calculated by Eq. (5).

Referring to Fig. 14 one observes that the percent variation in the abscissa $u_* d_s/\nu$ is the same as that in u_* and that the variation in the ordinate $\tau_o/(\gamma_s-\gamma)d_s$ is twice that in u_*. Based on the general considerations above, one may have an average error in the dimensionless shear stress of plus or minus 25 percent when this value is calculated by means of Eq. (8). When Eq. (5) is used the error is probably considerably less than this, and might be plus or minus 10 percent. In the opinion of the writer, the results using u_* from Eq. (5) are the more reliable.

On Fig. 14b the zones where different rates of transport were observed are marked. It is interesting to note that particle motion occurred over a large range of dimensionless shear stresses before critical motion was reached. For example the data for sand show that the ratio of critical shear stress to the lowest stress at which some motion was observed is approximately 1.5. For the glass beads, this ratio is approximately 3. This large range in stress which will produce a transport rate less than critical is an indication of the fluctuating nature of the fluid forces acting on the bed. The increase in transport rate as the shear stress increases results from an increase in frequency of the gusts of sufficient strength to move grains as well as in the strength of the gust, and hence, the number of grains per unit area which it moves. This relation is reflected in

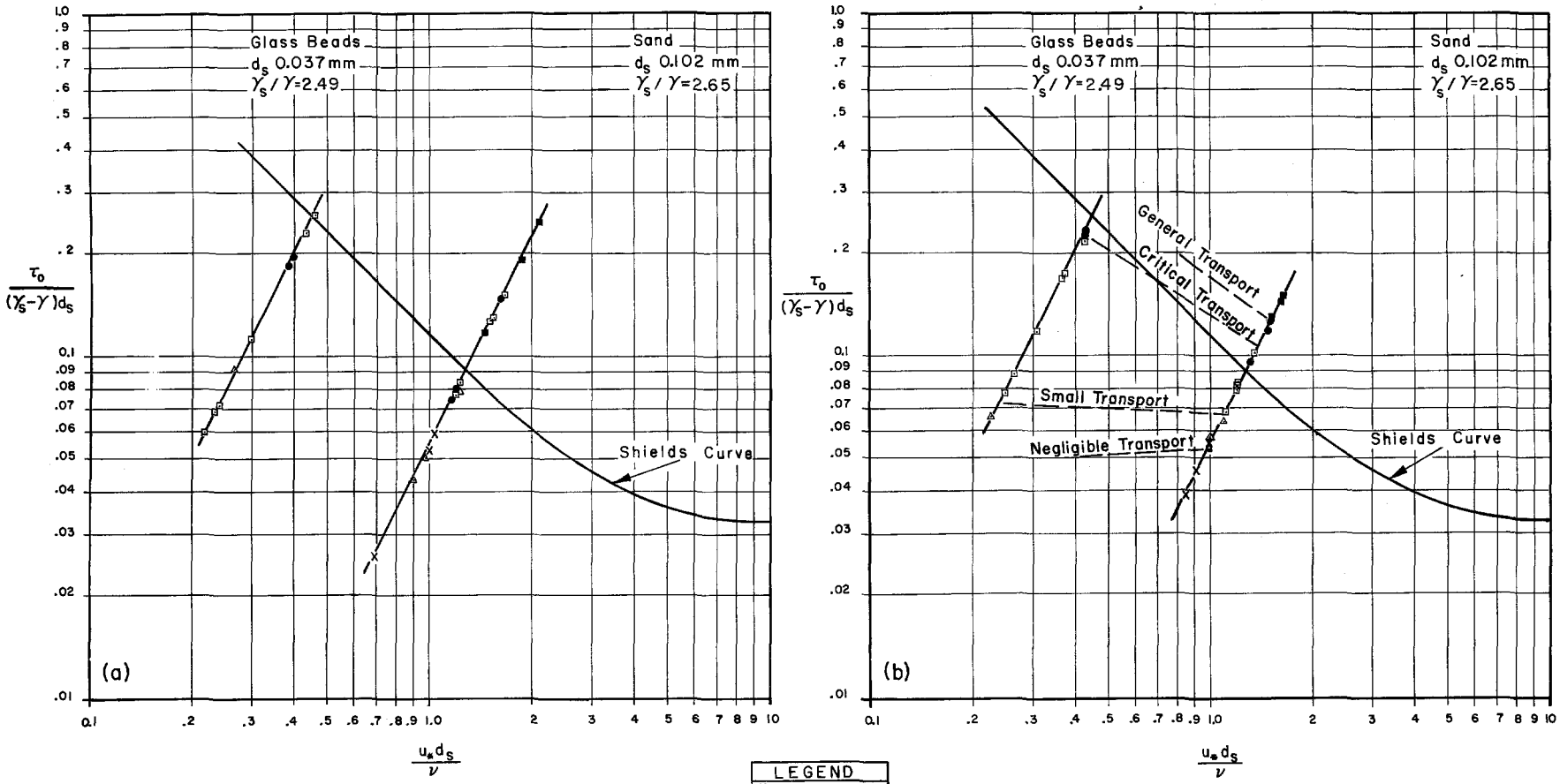

a) Calculations by Eq. (8).

b) Calculations by Eq. (5).

Fig. 14. Data for present experiments plotted on Shields graphs.

Table 2. The large range of shear stress over which "negligible" and "small" transport rates occur also indicates the difficulty of defining critical transport in a quantitative way. In view of this difficulty, it is remarkable that data of a single observer shows so little scatter, and it is even more remarkable that the data of several workers shown in Fig. 1 are so consistent.

The data for critical motion of sediment obtained in the present experiments by use of Eq. (5) have been plotted on a complete Shields graph in Fig. 15. On this same figure have also been plotted White's data for flows with turbulent boundary layers over a horizontal bed. It is at once apparent, as remarked earlier, that White's data give higher values of critical shear stress than those which determine the Shields curve.

Another interesting result is that White's critical shear stress for steel shot is considerably less than for the other materials. This can be attributed to the shape effect, which in White's analysis is accounted for by the angle of repose. White reported 0.685 and 1 respectively for the tangent of the angle of repose for steel shot and the sands in his experiments.

One can now interpret the results of the present experiments in the light of White's results. It is apparent that the data of White and of the present experiments define a reasonable curve on Fig. 15. This has been indicated by the dotted line labeled "Sands in turbulent boundary layer." This curve ignores the data point for steel shot because shot has a different shape than sand. For this same reason, the dotted curve was placed above the data points for the glass beads.

The fact that in Fig. 15 the data for sand and glass beads obtained in the present experiments agree reasonably well with the line with negative slope of unity proposed by Shields is inconsistent with the interpretation outlined in the preceding paragraph. In the opinion of the writer this suggests that the Shields curve gives excessive values of critical shear stress in this range. The evidence to support this idea, although not conclusive, is reasonable. The whole question points to the need for further experiments in this area. These should include experiments in flows with turbulent boundary layers in the entire range of boundary Reynolds numbers, and in flows with completely developed velocity profiles for boundary Reynolds numbers less than about 2.

As may be seen in Column 11 of Table 6 the values of the boundary Reynolds numbers range from 0.23 to 1.7. Since the thickness δ', of the laminar sublayer is given by

$$\delta' = 11.6 \frac{\nu}{u_*}$$

the ratio d_s/δ' given by $\frac{d_s}{\delta'} = \frac{1}{11.6}\left(\frac{u_* d_s}{\nu}\right)$ ranges from .020 to 0.15. Or in other words the laminar sublayer is from 7 to 50 sediment grain diameters in thickness. Because the grains are so thoroughly embedded in the laminar sublayer the only way that they can be exposed to a current sufficiently strong to move them is for the laminar layer to be swept away. The fact that the grains move in bursts indicates that the laminar layer is in fact swept away in bursts and that it then reforms. This intermittent removal and reforming of the laminar sublayer has been explored recently by Einstein and Li (8).

Einstein and Li observed the intermittency of the laminar layer by noting the motion of sediment grains in experiments similar to those reported herein. They also observed this phenomenon in flows in a smooth transparent pipe using dye injected through the wall to trace the flow. These authors derived the following expression for the time, T, for the laminar layer to develop once it has been swept away.

$$T = \frac{4}{\pi} \frac{u_e^2 \nu}{u_*^4} \qquad (11)$$

where u_e is the velocity at the edge of the laminar layer. In this development it was assumed that the time required to sweep away the laminar layer was small compared to the build-up time, T, and that the turbulent momentum exchange coefficient was large compared with ν resulting in a uniform velocity u_e in the turbulent core of the flow. Calculations of T for the experiments reported herein, using u_* calculated from Eq. (5) and u_o in place of u_e gave results of the same order of magnitude as the observed mean burst period for grain movement. The calculated values of T were also in agreement with observations in that these values diminish as the intensity of transportation increases. Calculated values of T for the conditions which produced critical movement ranged from 2.6 to 3.8 sec. while the observed period between bursts for critical movement was from 1 to 3 sec.

CONCLUSIONS

1. For the case of flows with a turbulent boundary layer, the data of the present experiments and those of White define a curve of dimensionless critical shear stress, $\tau_c/(\gamma_s - \gamma)d_s$ against boundary Reynolds number, $u_{*c}d_s/\nu$ as shown in Fig. 15.

2. For values of u_*d_s/ν in excess 2, where the Shields curve is defined by data, the curve for turbulent boundary layer gives higher values of critical shear stress than the Shields curve.

3. For values of u_*d_s/ν less than 2, the data from the present experiments agree rather closely with Shields curve, which in this range is extrapolated. This is inconsistent with the result for a larger u_*d_s/ν, presented in conclusion 2, and suggests that the extrapolated Shields curve gives excessive values of critical shear stress.

4. As a turbulent flow reaches conditions for incipient motion of sediment on the bed, it moves grains intermittently in gusts or bursts. The frequency of these bursts is correlated with number of grains per burst moving in a small area and can be used as a qualitative measure of transport rate, which is better than the purely visual estimate of transport used in most critical transport experiments.

5. The present experiments have demonstrated that for boundary Reynolds numbers less than 2 there is a wide range of shear stress less than the critical value for which some sediment movement occurs. This makes the critical shear stress difficult to define precisely.

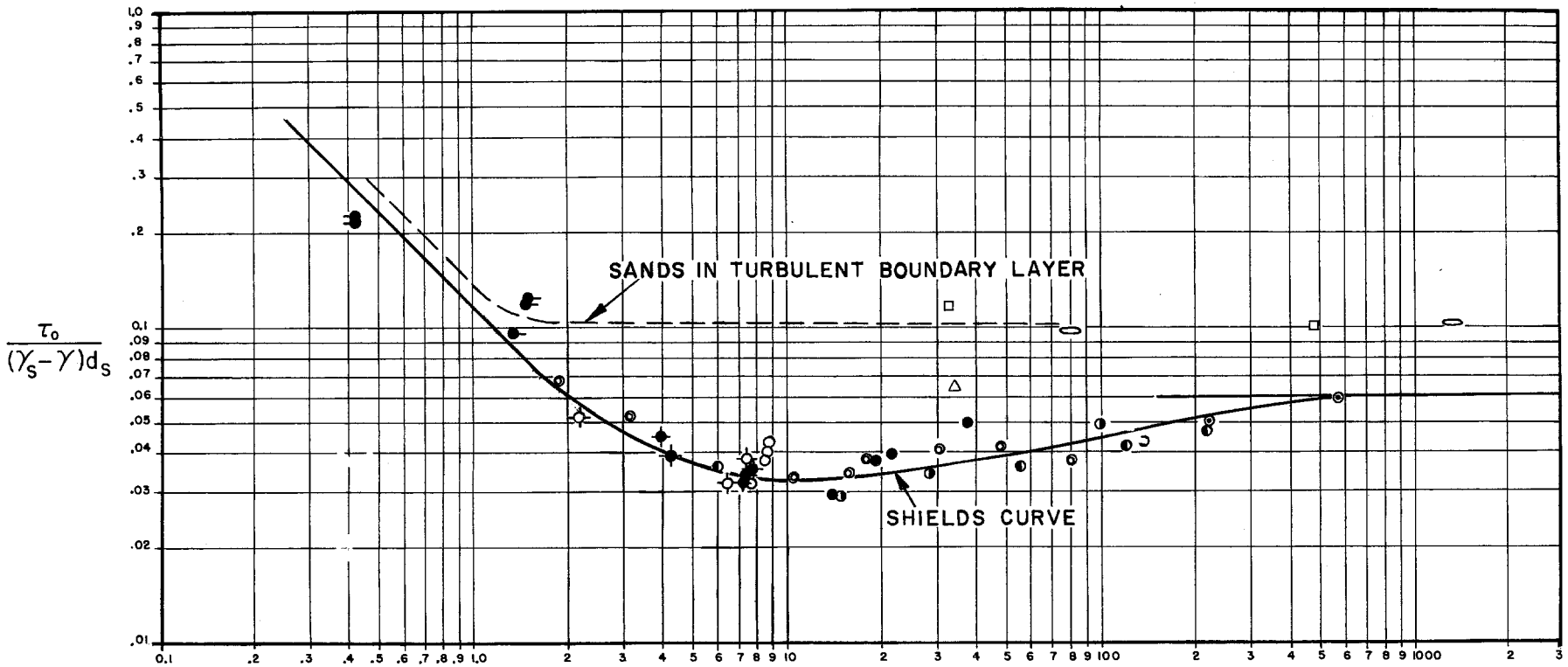

Sym	Description	γ_s-g/cm^3
○	AMBER	1.06
●	LIGNITE	1.27
◑	GRANITE (SHIELDS)	2.7
◐	BARITE	4.25
⊙	SAND (CASEY)	2.65
◇	SAND (KRAMER)	2.65
◆	SAND (U.S.W.E.S.)	2.65
◎	SAND (GILBERT)	2.65
⊷	SAND (VANONI)	2.65
⊸	GLASS BEADS (VANONI)	2.49
□	SAND (WHITE)	2.61
⬭	SAND IN AIR (WHITE)	2.10
△	STEEL SHOT (WHITE)	7.9

FULLY DEVELOPED TURBULENT VELOCITY PROFILE

TURBULENT BOUNDARY LAYER

Fig. 15. Shields diagram with data of White and of present experiments.

ACKNOWLEDGEMENTS

The main experiments reported herein were made by Antonio Bacalso, Assistant Research Engineer. Some of the preliminary experiments and the development of techniques used subsequently were carried out by Robert C. Y. Koh, Graduate Research Assistant. Arthur N. Schmitt, Research Technician, was responsible for designing and developing much of the special apparatus used, and assisted in carrying out some of the experiments. The construction and maintenance of the flume and other apparatus was carried out by Elton Daly, Laboratory and Shop Supervisor, and Robert Greenway, Laboratory Mechanic.

The project was supported by U. S. Public Health Service Grant RG-6915.

APPENDIX I

NOTES ON MOTION PICTURE (Ea-3-I)

Entrainment of Fine Sand in a Turbulent Boundary Layer

Entrainment of Fine Sand in a Turbulent Boundary Layer

(16 mm black and white film, silent with titles. Taken at 64 frames per sec Length 225 ft)

1. General Description of Film

This motion picture was taken to show the nature of incipient motion of sediment grains in a flow with a developing turbulent boundary layer. The pictures show a small portion of the sediment-covered bed about 12 mm long by 10 mm wide. All pictures were taken at 64 frames per sec. Therefore if they are projected at 16 frames per second the motion will be speeded up four times and if they are shown at 24 frames per second the motion will be speeded up somewhat less than three times. The sediment in all runs is quartz sand with a geometric mean size of 0.102 mm and a geometric standard deviation of 1.14 (see Fig. 10 for size-frequency distribution). The flume in which the experiments were made has glass sides and is 15-3/8 inches wide and 14 ft long (Fig. 3). The water is baffled in the inlet tank and is introduced into the flume with a low turbulence level and a uniform velocity.

The scenes in the picture were all taken in flows 0.391 ft deep with mean velocities ranging from 0.71 to 1.0 ft per sec. The motion pictures were taken on the centerline of the flume, at stations 3, 5, and 10, that is, 3, 5, and 10 feet from the flume inlet. At station 10 the boundary layer was always completely turbulent. The transition of the boundary layer from laminar to turbulent flow occurred between stations 3 and 5 so that at these stations the flow alternated between being laminar and turbulent. Observations were made in four different flows. In two of these all conditions corresponded to those for runs R-3 and R-4 described in the main report. In the other two when the discharge was increased beyond that of runs R-3 and R-4 the flow conditions exceeded those for initiation of sediment movement and ripples had formed on the bed.

The film contains 11 scenes and 13 titles as indicated in Table I which follows. The number of the scene appears on the film in parenthesis at the beginning of the title for each scene. The first and third titles apply to the film in general. The conditions for each scene are also shown in Table I.

Table I. Description of Motion Picture

Scene No.	Run No.	Sta. (ft)	Mean Vel. ft/sec	Bound. Layer Thick. ft	Ratio of Sed. Size to Thick. of Lam. Sublayer d_s/δ'	Condition of Flow in Boundary Layer	Intensity of Sediment Movement
1			0	-	-	-	None
2			0	-	-	-	None
3	R-3	10	0.71	0.15	0.10	Turbulent	Small
4	R-4	10	0.82	0.13	0.12	Turbulent	Critical
5	R-4	5	0.82	-	-	Transition	Small
6	R-3	5	0.71	0.065	-	Transition	Negligible
7	R-3	3	0.71	-	-	Transition	None
8	R-4	3	0.82	-	-	Transition	Small
9	R-4	10	0.82	0.13	0.12	Turbulent	Critical
10		10	0.88	-	-	Turbulent	General
11		10	1.00	-	-	Turbulent	General

It is pertinent to note that at station 10 in runs R-3 and R-4 the ratio d_s/δ' of the sediment size, d_s(0.103 mm) to the thickness of the laminar sublayer δ' is 0.10 and 0.12 respectively. This means that δ' was about 8 to 10 times the grain size, and that the grains were well submerged in the laminar layer. It also means that in order to move grains the laminar layer must be penetrated by currents from above and shows that this layer is intermittent rather than remaining steady as inferred by many treatments of this problem.

2. Detail description of film

1st Title

Entrainment of fine sand in a turbulent boundary layer
W. M. Keck Laboratory of Hydraulics and Water Resources
Division of Engineering and Applied Science
California Institute of Technology
February 1962
Prepared under U. S. Public Health Service Grant RG-6915

2nd Title

(1) Still bed

Scene 1

3rd Title

Bed material is quartz sand
Mean size: 0.102 mm
Flume: 15-3/8 in. wide by 14 ft long
Water depth: 0.391 ft
Taking speed: 64 frames per sec

4th Title

(2) Millimeter scale shows field of view

Scene 2

5th Title

(3) Run R-3 station 10
Mean velocity 0.71 ft per sec
"Small" transport

Scene 3

Comment: In this scene the fluid forces on the sand particles in the bed are smaller than needed to produce what has been defined as beginning of movement. The motion is infrequent and only a few grains are moved in each burst of motion. The rate or intensity of sediment motion at or near conditions for incipient motion has been described qualitatively as "Negligible", "Small", "Critical", and "General." By definition the critical intensity corresponds to incipient motion. In this scene the motion is considered to be "Small", the boundary layer thickness $\delta = 0.15$ ft and the ratio of the sediment size, d_s to laminar sublayer thickness δ is $d_s/\delta = .10$. The low value of d_s/δ' indicates that the grains are well submerged in the laminar sublayer. In order for the grains to be exposed to a current strong enough to move them the laminar layer must be penetrated by the fluctuating currents in the turbulent flow near the bed.

6th Title

(4) Run R-4 station 10
Mean velocity 0.82 ft per sec
"Critical" transport

Scene 4

Comment: The motion is still intermittent although the burst frequency and the number of grains moved per burst are higher than in the previous scene. At this station $\delta = .130$ and $d_s/\delta' = 0.12$.

7th Title

(5) Run R-4 station 5
End of transition region
"Small" transport

Scene 5

Comment: This scene is taken at the downstream end of the transition region where the flow changes from being turbulent part of the time to being always turbulent. The rate of transport, although slightly less than in Scene 4 is considered to be "Small" instead of "Critical" as in Scene 4.

8th Title

(6) Run R-3 station 5
End of transition region
"Negligible" transport

Scene 6

Comment: This scene like the previous one is taken at the downstream end of transition region. The transport rate is definitely less than in Scene 5 because the mean velocity and hence the forces acting on the bed are smaller. Careful visual observations showed that the rate of transport was also less than at stations 10 further downstream in the same flow. However this is not obvious from a comparison of Scenes 3 and 6. To bring this out in motion pictures the scenes need to be made longer.

9th Title

(7) Run R-2, station 3
Beginning of transition region
No transport

Scene 7

Comment: This scene was taken at the upstream end, i.e., at the beginning of the transition region. At this position turbulence occurs only infrequently. No turbulence of sufficient intensity to move grains occurred during this scene.

10th Title

(8) Run R-4 station 3
Beginning of transition region
"Small" transport

Scene 8

Comment: A few frequent bursts occur at the beginning of this scene and then motion ceases completely. This illustrates the fact that at the beginning of the transition region in which the change occurs from laminar to turbulent flow, turbulence occurs infrequently.

11th Title

(9) Run R-4 station 10
Completely turbulent flow
"Critical" transport

Scene 9

Comment: This scene is for the same conditions shown in Scene 2 and is repeated to help the viewer compare critical motion with lesser rates of motion.

12th Title

(10) Station 10
Mean velocity 0.88 ft per sec
"General" transport; ripples on bed

Scene 10

Comment: The mean velocity has now been increased from 0.82 ft per sec in runs R-4 to 0.88 ft per sec; the rate of sediment motion has been increased from "Critical" to "General" and ripples have formed on the bed.

13th Title

(11) Station 10
Mean velocity 1.0 ft per sec
"General" transport; ripples on bed

Scene 11

Comment: The velocity has been increased to 1.0 ft per sec, ripples have formed in the bed, and the transport rate has also increased.

BIBLIOGRAPHY

1. Shields, A., "Anwendung der Aehnlichkeitsmechanik und der Turbulenzforschung auf die Geschiebebewegung," Mitt. der Preuss. Versuchsanstalt für Wasserbau und Schiffbau, Berlin, 1936.

2. Rouse, Hunter, "An analysis of sediment transportation in the light of fluid turbulence," U. S. Dept. of Agric., Soil Cons. Service SCS-TR 25, July 1939.

3. White, C. M., "The equilibrium of grains in the bed of a stream," Proc. Royal Soc. A., Vol. 174, 1940, pp. 324-338.

4. Kramer, Hans, "Sand mixtures and sand movement in fluvial models," Trans. Amer. Soc. of Civil Engrs., Vol. 100, pp. 798-878, 1935.

5. USWES, "Studies of river bed materials and their movement with special reference to the lower Mississippi," Paper 17 of U. S. Waterways Experiment Sta., Vicksburg, Miss., Jan. 1935.

6. Vanoni, Vito A., and Brooks, Norman H., "A study of turbulence and diffusion using tracers in a water tunnel," Report E-46, Hydrodynamics Lab., Calif. Inst. of Tech., Jan. 31, 1955.

7. Tsien, Hsue-Shen, "On the design of the contraction cone for a wind tunnel," Jour. Aero. Sci., Vol. 10, No. 2, pp. 68-70, Feb. 1943.

8. Einstein, Hans A., and Li, Huon, "The viscous sublayer along a smooth boundary, Trans. Amer. Soc. of Civil Engrs., Vol. 123, pp. 293-317, 1958.